Final Year Project Report Titled

"Development of a Generalized Stochastic Microcontact Model for Friction Coefficient of Elliptical Contacts Operating in the Mixed EHL Regime"

Submitted
in partial fulfillment of
the requirements of the degree of
Bachelor of Technology in Mechanical Engineering

By
Samir Kadri - 201020005
Siddharth Sankhe - 201020013
Madhusudhan Kulkarni – 201020027
Rohan Adkhale – 201020031
A.Y. 2023- 2024

Dr. Mandar Tendolkar
VJTI - Guide / Supervisor

Dr. David Talbot
Dr. Isaac Hong
Ohio State University, USA – External Guide

Department of Mechanical Engineering
Veermata Jijabai Technological Institute
Mumbai 400 019
A.Y. 2023-2024

CERTIFICATE OF COMPLETION

THE OHIO STATE UNIVERSITY

Project Completion Certificate

Final Year Undergraduate Project

Siddharth Sankhe,
Samir Kadri
Rohan Adkhale
Madhusudhan Kulkarni

VJTI (Veermata Jijabai Tech. Institute), Mumbai

for the successful completion of their final year undergraduate project (under the guidance of Professors D. Talbot and I. Hong in the telecommuting mode) on a project entitled "Development of a Generalized Stochastic Microcontact Model for Friction Coefficient of Elliptical Contacts Operating in the Mixed EHL Regime".

Assistant Professor
David Talbot

Research Assistant Professor
Isaac Hong

ACKNOWLEDGEMENT

We would like to use this opportunity to thank everyone who has helped us during the final year project. Firstly, we extend our gratitude towards GEARLAB advisors, Prof. David Talbot, and Dr. Isaac Hong who has worked alongside the team and has been instrumental in helping us complete our project. Dr. Isaac and Prof. Talbot's encouragement and guidance throughout each session were invaluable, and we look forward to seeking their guidance in the future too. We also wish to thank the entire GEARLAB and the contributors towards the Windows LDP application, which is truly a state-of-the-art software for gear modelling. We would also like to thank Dr. Rajendra Singh, who co-ordinated and helped us to connect with the faculties of OSU for this project. We would also like to thank Dr. Mandar Tendolkar, who endorsed us for the project at GEARLAB and has been constantly supporting and guiding us. We would also like to thank our friends and family for their confidence in our abilities and for making sure that we had fun along the way.

ABSTRACT

The report presents the research conducted on the design and modification of Stochastic microcontact model which implies the use of statistical approximations along with the formulations to compute the power loss. Losses associated with this are majorly of two types: Load Dependent losses (Mechanical) and Load Independent losses (Spin). Mechanical losses in our model represent the sliding frictional force that occurs due to the asperity contact and EHL (Elasto-Hydrodynamic Lubrication) conditions of the contact. Gear roughness surface profiles, gear geometry, operating conditions, and lubricant properties all affect the mechanical losses. These power loss models can be bifurcated into two types based on how they calculate the results, 1) Deterministic model, where all the parameters such as local pressure, fluid, temperature, and roughness conditions are analysed in high resolution discretization of the contact and time variant behaviour such as models by Li and Kahraman [1]. 2) Stochastic model uses empirical and simulated estimations of macro pressure, fluid temperature and roughness contact conditions along with Greenwood-Williamson (GW) microcontact model [2]. The deterministic models are accurate but computationally expensive. The GW based models allow for rapid calculation but are limited in validation against experimental results under wide varieties of gear operating conditions and surface roughness types. Entire working of the Stochastic model can be divided into two parts, the first part is the gear model which used the above-mentioned parameters to compute the effective viscosity and the effective friction coefficient for asperity contact ratio and EHL [4]. The Greenwood Williamson model [2] is a formulation that is used to parameterize the roughness profiles of the gear tooth surface. Results for the generalized model were verified with the results of the earlier stochastic model for the spur gears along with the measured data and the results of Li and Kahraman's deterministic model. For helical gears, the measured data was obtained from Vaidyanathan's thesis [5]. The second module focuses on the estimating power losses for any two contacting surfaces using the B.J. and Hamrock formulation [16] for computing film thickness, contact pressure. Using the formulations, we can calculate power losses for different ratios of sliding to rolling velocity. Using Shon's thesis [17], results were verified. Results obtained were in line with the desired error range and they follow the trend as expected. Newer model was faster in computation and smaller in size compared to the initial model and yielded same results.

Keywords: Line Contact, Elliptical Contact, Elasto-Hydrodynamic Lubrication, Piezo-Visco-Elasticity, Greenwood Williamson model

TABLE OF CONTENTS

LIST OF FIGURES

LIST OF TABLES

LIST OF ABBREVIATIONS

EHL = Elastohydrodynamic lubrication

WindowsLDP = Windows Load Distribution Program

W = Load Parameter

G = material parameter

U = Speed parameter

$\boldsymbol{\alpha}$ = Pressure Viscosity Coefficient

hmin - Film thickness

$\mathbf{p_c}$ - Maximum Contact pressure

R - Effective radius

K - Ellipticity ratio

α - Pressure viscosity coefficient

η* - Effective viscosity

$\mathbf{u_1}$ = Velocity of roller

$\mathbf{u_2}$ = Velocity of disc

Ø1 = Roll angle

μ = effective friction coefficient of the contact

m0 = 0th Fourier coefficient

m2 = 2nd Fourier coefficient

m4 = 4th Fourier coefficient

E' = Equivalent Young's modulus

ÛR = Average rolling velocity

$\boldsymbol{\eta*}$ = Effective lubricant velocity

a = Hertz contact radius

μB= boundary friction coefficient

μE = EHL (Couette) friction coefficient

PB = boundary friction area of contact

PE = EHL friction area of contact

$\mathbf{u_s}$ = Sliding velocity

$\vec{\mathbf{u}}$ = Average effective friction coefficient over one mesh cycle of gear

$\vec{\mathbf{U}}_\mathbf{s}$ = Average sliding velocity over one mesh cycle of gear

Fm = Mesh force

$\mathbf{U_R}$ = Rolling Velocity

η = Lubricant viscosity

A = Asperity Contact Area

ISF = Isotropic Superfinishing

τ = Total shear stress.

τ_y = Yield Stress

γ = Shear rate.

$\mathbf{w_p}$ = Distance of points in overlapping region

CHAPTER ONE: INTRODUCTION

1.1 INTRODUCTION

Tribology [1] is a vital field in the design of mechanical systems; it deals with engineering related to the understanding and management of friction, lubrication, and wear phenomena of two interacting surfaces. The fundamental objects of study in tribology are systems that consist of at least two contacting bodies and any environmental factor that affects their interaction. The field of mechanical engineering relies on numerous tiny parts working together as a system. The performance of the system as a whole hinge on how these numerous elements interact with one another. It has been known for thousands of years that surfaces brushing and colliding with one another harm the constituent parts. At first, this damage might not be noticeable, but over time, it could cause mechanical failure. The study of tribology explains why this harm happens and how mechanical engineers could mitigate it.

For the same reason, in order to design an optimal transmission system, it is vital to ensure that the power losses that contribute to heat generation and losses in efficiency are carefully considered when developing the system's transmitting components. These power losses are characterized into three types: friction, wear, and lubrication. Friction is the force that resists the motion of two contacting surfaces with relative motion, and depends on the coefficient of friction of these two interacting surfaces. Friction will always exist in a system which possesses interacting components with relative motion, however it is preferable to have as little friction as feasible. Even in the best-case scenario, the system dissipates energy as heat as a result of the friction. Excessive friction can put a component under a lot of shear stress and cause wear which eventually leads to failure. The term "wear" describes the material loss that occurs when two or more components brush against one another. Abrasive wear and Adhesive wear are the two primary categories of wear. When the tougher surface wears away at the softer one it slides against, abrasive wear takes place. Conversely, adhesive wear happens when the surfaces adhere to one another while sliding, resulting in material loss on one surface. A third failure method of wear occurs after, when a system undergoes multiple cycles of the same load enough times it eventually fails, despite the stress it is subject to is lower than its ultimate tensile strength. This is brought on by tiny flaws in the part that generate microscopic fissures that are invisible to the naked eye. Even if these cracks are not problematic at first, they will spread and deepen because of repeated cycles of this stress. The point at which these fissures enlarge to the point that the system fails as a whole is known as fatigue failure. It is advantageous to make

sure that a system's components can slide across one another and interact with little—or ideally, no resistance to minimize wear. It is best to make sure that the surfaces of each component do not come into direct contact at all during sliding to limit the danger of wear; this is brought about with the use of lubrication. More than merely wear and friction are resolved by proper lubrication. In addition to addressing these two problems, lubrication also controls temperature since elevated temperatures can cause machine parts to deform plastically. Certain lubricant types will also shield surfaces from corrosion and rust.

There are other considerations to take into account when lubricating sliding surfaces. Depending on the situation, different lubricating films need to be used. Boundary, mixed, and hydrodynamic lubrication are the three primary "regimes" of lubrication. Boundary lubrication refers to the regime with the smallest thickness, and leads to extremely little separation between the two interacting components, and is typically used in conditions with slow speeds and short stress cycles. Conversely, hydrodynamic lubrication takes place at the other extreme. This regime is observed when the machine is required to operate constantly with little stopping and starting and the sliding is happening at a very high speed. The film thickness reaches its maximum in this regime; in fact, there is no contact at all between the two sliding surfaces. Mixed lubrication is a combination of the two, where the two interacting surfaces occasionally touch.

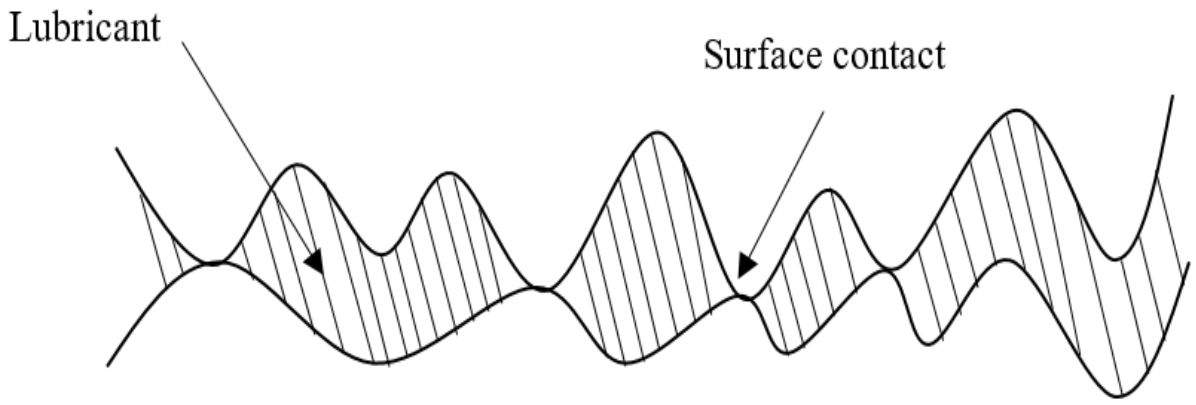

Figure 1.1: Contact between two surfaces [2]

This research seeks to generate a stochastic power loss model using surface asperity profiles with simplified Elastohydrodynamic lubrication (EHL) metrics to calculate the effective friction coefficient in mixed lubrication gear (spur and helical) and elliptical contacts. Power loss experiments described in referred literature were then used to validate the results generated by the model by comparing them to the experimental findings. Some of these metrics are

outputs from Ohio State University's proprietary software: WindowsLDP. WindowsLDP is combination of large datasets of experimentally acquired power loss values for a very large pool of gear types and different conditions of torques and speeds. This enormous dataset is then statistically fitted into a characteristic equation using regression. However, in order to fit the value in regressed equation and to have a less complex regressed equation, some of the accuracy of the power loss values is compromised. The stochastic model does real time computation instead of fetching the best value from the regressed equation.

1.2 OBJECTIVE 1

The overall goal of this project is to develop a stochastic (probabilistic) model to compute the mesh or the sliding losses that are caused due to the meshing of gear tooth (line contact) or due to interaction of any two surfaces (elliptical contact). The entire project can be divided into 2 objectives based on the type of contact i.e., line or elliptical contact.

Goal: To create a 3D stochastic model [4] that eliminates the issues found in the 2D stochastic model and expands the domain of the model from spur to helical gears [5], thereby increasing the accuracy and compatibility of the stochastic model (i.e., generalization). Validate the power loss data obtained from the stochastic model using the measured data [5].

The 2D stochastic model focused solely on the time and contact points on the centerline of face width along the Line of Action, whereas the 3D stochastic model focuses on all contact points present in the contact region generated by the Line of Action and the face width. The third dimension is time, or timestep. A timestep is the amount of distance travelled along the Line of Action in a single unit of time. This was necessary because the software (WindowsLDP) [7] used to generate the required inputs for the stochastic model encountered a numerical limit for the helical gears, reducing the model's accuracy when compared to measured power loss values. To address this issue, we needed to implement the concept of a 3D stochastic model, and in addition to resolving WindowsLDP issues, we wanted to improve the model's accuracy for spur gears. To validate the power loss values calculated by the stochastic model, we use power loss values generated by WindowsLDP, which uses a large database of experimentally calculated

power loss values obtained through statistically regressed equations. We also have measured power loss values that are calculated using the experimental setup explained in the chapter 2.

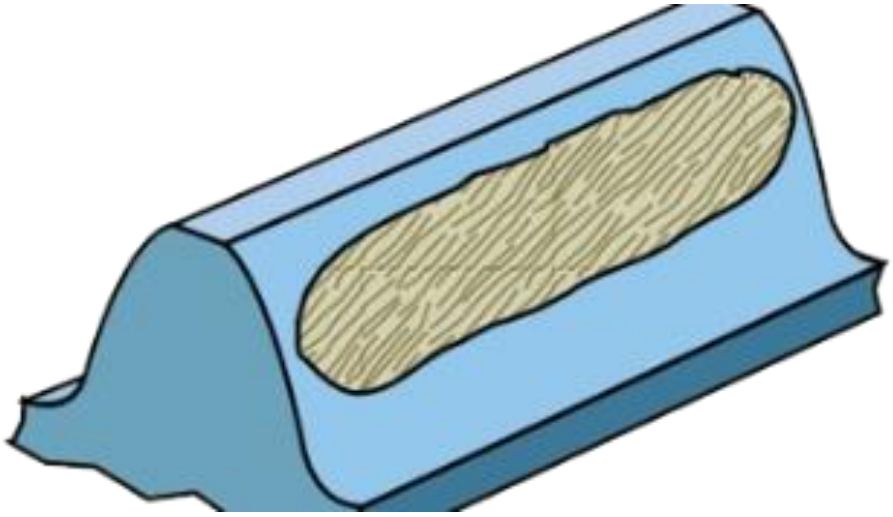

Figure 1.2: Gear Tooth Contact Region - Spur Gear [13]

1.3 OBJECTIVE 2

Goal: To develop a generalized model to further predict elliptical contact found in twin-disk and ball on disk tribometers [16]. This involves generating new load distribution section of the model where a formulation for the contact pressure, film thickness, and sliding velocity need to be described and made compatible with the rest of the stochastic Microcontact model [18]. Model results are to be compared to the twin disk tribometer measurements made at OSU [17].

Although the gear power loss model was designed for a specific use case, a more generalized model that could be applied to any type of surface in contact which this model treats as elliptical contacts was required. Since the generalized model with elliptical contact does not lend itself to formulations of line contact, a fresh set of formulations needs to be integrated to the stochastic model. The model forecasts the power loss for the specified contacting surface at a single point of contact between two surfaces by formulating the contact pressure, film thickness, and sliding velocity at that location. The model is built on the formulas that produce the most accurate results, and these formulations are validated using the experimental values using the experimental setup explained in chapter 2.

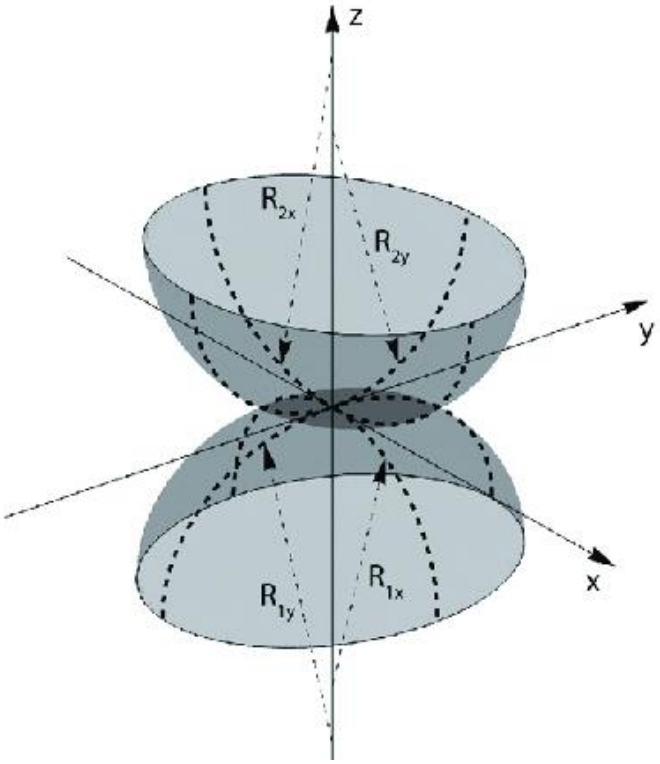

Figure 1.3: Demonstration of Elliptical Contact - these surfaces usually have crowning [19]

1.4 ASSUMPTIONS

- Boundary friction coefficient (u_B) is constant for all the conditions of torque and speed. (Boundary friction coefficient value is found out using practical tests with a large range of datasets and the value was nearly constant for all the tests and hence the value is assumed to be u_B) [4]
- Asperity height is assumed to follow gaussian distribution, uniform asperity density and tip radii. [4]
- Fluid (EHL) and dry sliding (asperity contact) components are assumed to be independent. [1]
- Elastic hysteresis is assumed to be negligible.
- Roughness values of measured and model data may have a difference up to 25%.

1.5 THESIS ORGANIZATION

Chapter One: Introduction

Introduction to the research topic and objectives.

Chapter Two: Literature Review

Review of existing theories and formulations related to lubrication regimes and contact models.

Chapter Three: Model Development

Description of the 3D stochastic model and methodology for elliptical contact modeling.

Chapter Four: Results And Discussions

Presentation and discussion of results for gear power loss and elliptical contact power loss models.

Chapter Five: Conclusions And Future Scope

Conclusions drawn from the models developed and suggestions for future research directions.

CHAPTER TWO: LITERATURE REVIEW

The total power loss in mixed lubrication contacts used to transmit power is a combination of various types of losses; such as fluid film sliding loss, rolling loss, dry friction loss and losses due to elastic hysteresis [1]. This research focuses on creating a model to predict the effective friction coefficient in the mixed lubrication contacts.

Literature on the Mixed EHL Regime describes it as the type of lubrication that has both, the boundary lubrication (asperity contact or contact friction) and hydrodynamic lubrication present. Both the lubrications contribute towards the effective friction coefficient and the friction acting on the system. This is calculated using the Tallian's Load Sharing approach [3].

The paper authored by I. Hong, E. Aneshansley, K. Chaudhary & D. Talbot describes a stochastic model developed that is capable of making estimates of mechanical power loss in gears [4]. This literature serves as the inspiration of the conducted research and is used to extend the work to not only gears (spur and helical) but also elliptical contacts.

I. Hong, E. Aneshansley & D. Talbot's work on the design calculations and methods used to interpret gear losses due to sliding friction and losses due to surface contact was integrated into the section of the code that deals with predictions for spur gears. Methods such as Mccool's parameterization method [11] to determine 2D roughness profiles, Hertzian pressure distribution to calculate the maximum contact pressure of an elliptical pressure distribution and Tallian's load Sharing approach are included in the literature and used to effectively make the required calculations, while also providing reference for necessary assumptions for the same [12]. This was used along with data extracted from the WindowsLDP load distribution program, which is a stochastic model that uses regressed equations derived from deterministic model data. The model also served as a tool to sufficiently understand the behaviour and shape of contact patches in the various gears [2]. This was further expanded into the section for helical gears, for which equations used to determine and power losses were referred to from A. Vaidyanathan's work [5]. The thesis focused on calculating the power loss of helical gears. Along with the mathematical expressions used to theoretically calculate the power loss of helical gears, the thesis also shows the schematics for creating a test setup to calculate power losses experimentally. The thesis also serves as a reference point because the gear geometry is based on Vaidyanathan's thesis, and the experimental power loss values for the torque and speed losses are used to validate the stochastic model's predicted power losses. The thesis also

provides a clear differentiation on the sliding and the rolling losses in the gear and the test setup design also helps us to easily discretize the power loss based on sliding and rolling losses. For sliding losses, the stochastic model is used based on the Greenwood Williamson model and Tallian's Load Sharing Approach and for the rolling losses, Palmgren Formulation is employed in the thesis [2].

The final objective of the paper, aiming to develop a section that makes the same estimations for elliptical contacts, was achieved by using equations from R. J. Chittenden, D. Dowson, J.F Dunn, C. M. Taylor's work outlined in a two part publication, which outlines formulations such as the B.J. Hamrock and D. Dowson Formulation for the calculation of minimum film thickness for EHL Elliptical contacts with crowning, formulations for rolling and sliding velocities between two disc at different velocities, and various other equations essential to approach towards the final result, as well as the basis algorithm for the model [16] ; along with J. A. Greenwood's work titled Analysis of Elliptical Hertzian Contacts, which is used to calculate the maximum contact pressure of an elliptical pressure distribution for elliptical surfaces in contact [8]. Datasets for two lubricants, 80W90 and MIL PRF 23699, available in a paper authored by S. Shon were used to generate results at various values of contact stress. The literature focused on friction, scuffing and wear characteristics of elliptical contacts and depicts the entire methodology and test set up used for the conducted experimentation. The results generated using the data from the paper in the generated model were then validated against the corresponding results obtained by the author of the same paper [17].

2.1 LUBRICATION REGIME [13]

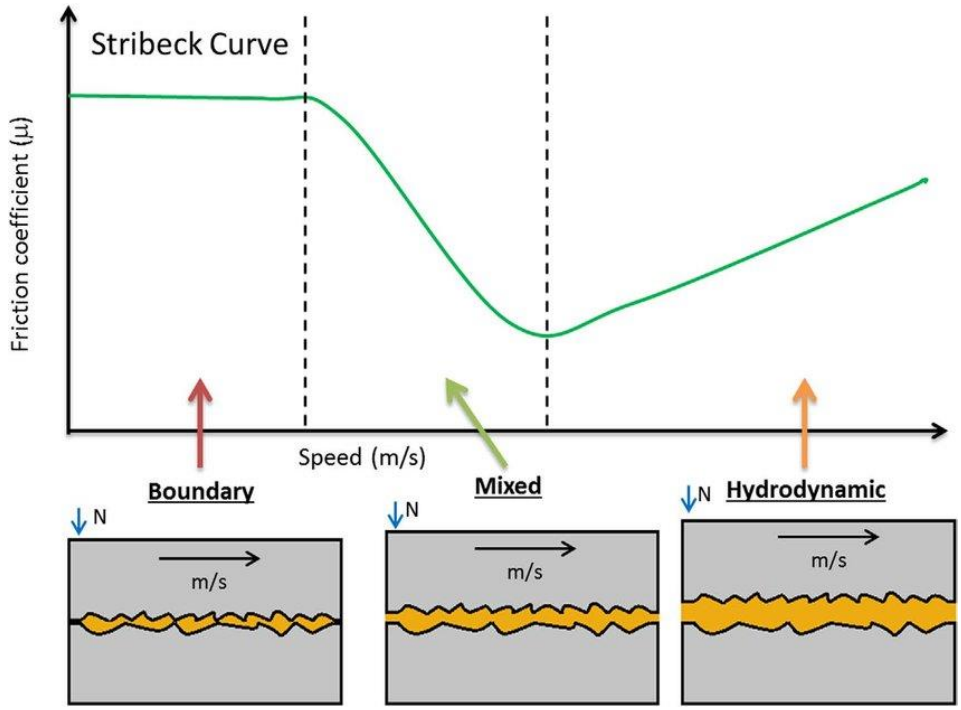

Figure 2.1: A Stribeck curve and illustrations of the 3 lubricant regimes [13]

The Stribeck curve is a fundamental concept in tribology, the study of friction, wear, and lubrication. It graphically represents the relationship between the coefficient of friction and a lubrication parameter. This parameter is a combination of the lubricant's viscosity, the relative velocity between the contacting surfaces (sliding velocity), and the normal load acting on the contact area. This parameter can also be replaced by sliding velocity as shown in the figure 2.1 or minimum (central) film thickness. Stribeck curve captures the non-linear behaviour of the friction in a lubricated system and this delineates into three distinct lubrication regimes [15].

1. **Boundary Lubrication**

   Boundary lubrication happens at low speeds or high loads. The lubricant film is too thin to fully separate the microscopic peaks (asperities) on the contacting surfaces. When these asperities come into direct contact, there is a lot of friction. Boundary lubricants frequently include additives that create a protective layer on the surfaces, reducing wear. This regime is critical for machine startup and shutdown, as well as in slow-moving, heavily loaded components.

2. **Mixed Lubrication**

   Mixed lubrication is an intermediate zone between boundary and hydrodynamic lubrication. It occurs when operating conditions (speed or load) start to change. Friction

varies according to the specific conditions. As the thickness of the lubricant film increases with changes in speed or load, friction decreases to hydrodynamic levels. Mixed lubrication, like boundary lubrication, can benefit from lubricants containing film strength and anti-wear additives. This regime is common in many operating conditions, particularly during startup and shutdown, or when operating loads or speeds change.

3. **Hydrodynamic Lubrication**

   Hydrodynamic lubrication is the optimal regime, occurring at high speeds or low loads. The lubricant film is thick enough to separate the asperities on the contacting surfaces, which prevents metal-to-metal contact. The complete separation of surfaces results in minimal friction. The viscosity of the lubricant is very important here. A higher viscosity lubricant forms a thicker film under a given operating condition, promoting hydrodynamic lubrication. This regime is critical in high-speed bearings, journal bearings, and other components where friction and wear are minimised.

Our focus will be on the mixed lubrication regime where the contact shall comprise of asperity contact and lubrication film operating in the piezo-viscous-elastic (VE) regime. In our case, we shall observe that the system will lean towards boundary lubrication at lower speeds and at higher speeds, the system will tend to move towards the hydrodynamic lubrication. Thus, it is beneficial that the Stochastic model tends to stay in the mixed lubrication regime as loads fluctuate and net effective friction coefficient is low for mixed lubrication regime. The Stribeck curve traditionally covers three lubrication regimes, but there is another one called the piezo-viscous-elastic (VE) regime that applies under specific conditions.

2.2 PIEZO-VISCO-ELASTIC REGIME [4]

This regime comes into play when extremely thin films (nanometres) separate contacting asperities. In these cases, the lubricant behaves differently than a typical viscous liquid. The name piezo-viscous-elastic reflects two important aspects: The term piezo-viscous refers to a lubricant's viscosity that increases with pressure. Elastic refers to the fluid's ability to exhibit elasticity while remaining viscous at these small scales. The VE regime is typically characterised by very smooth surfaces, minimal asperities, extremely thin film thicknesses, and specialised lubricants designed for these conditions. Friction behaviours in this regime can be complex and diverge from the Stribeck curve. Increased film thickness may not result in as significant friction reduction as hydrodynamic lubrication.

2.3 LINE CONTACT (HERTZIAN THEORY) [14]

In mechanics, when two bodies make contact, the actual area of contact is frequently much smaller than the apparent area due to surface roughness and irregularities. Line contact reduces the contact area to a single line. This scenario is common in many engineering applications, including the design of gears, bearings, and rolling contact elements. Line contact analysis involves examining the distribution of forces, stresses, and deformations along the contact line. Line contacts occur between two surfaces that are flat along one axis but curved along the other. One or both surfaces may be curved (parallel cylinders or a cylinder on a flat). The surfaces may also be concave (negative radius) or convex (positive radius). Any two surfaces that are curved along one axis but straight and parallel along the other can be converted into a rigid cylinder contacting a flat elastic half space. This contact will exhibit a distinct pressure profile and stress distribution.

Hertzian line contact theory describes how applied loads are distributed along the contact line. It predicts a characteristic pressure distribution, similar to Hertzian spherical contact theory, with the highest pressure at the centre of the line and decreasing pressure towards the edges. The pressure distribution is determined by factors such as the geometry of the contacting bodies, the applied load, and the material's elastic properties. Under the applied load, the contacting bodies elastically deform to accommodate the pressure distribution. Hertzian line contact theory offers equations for calculating the deformation of bodies along the line of contact. This deformation is critical in determining factors such as the contact area, the extent of elastic deformation, and the stresses generated within the bodies. The theory also allows for the calculation of stress distribution within contacting bodies. It predicts how stress changes along the line of contact and provides information about critical areas where stress concentrations may occur. Understanding stress distribution is critical for assessing the structural integrity and fatigue resistance of components subjected to line contact.

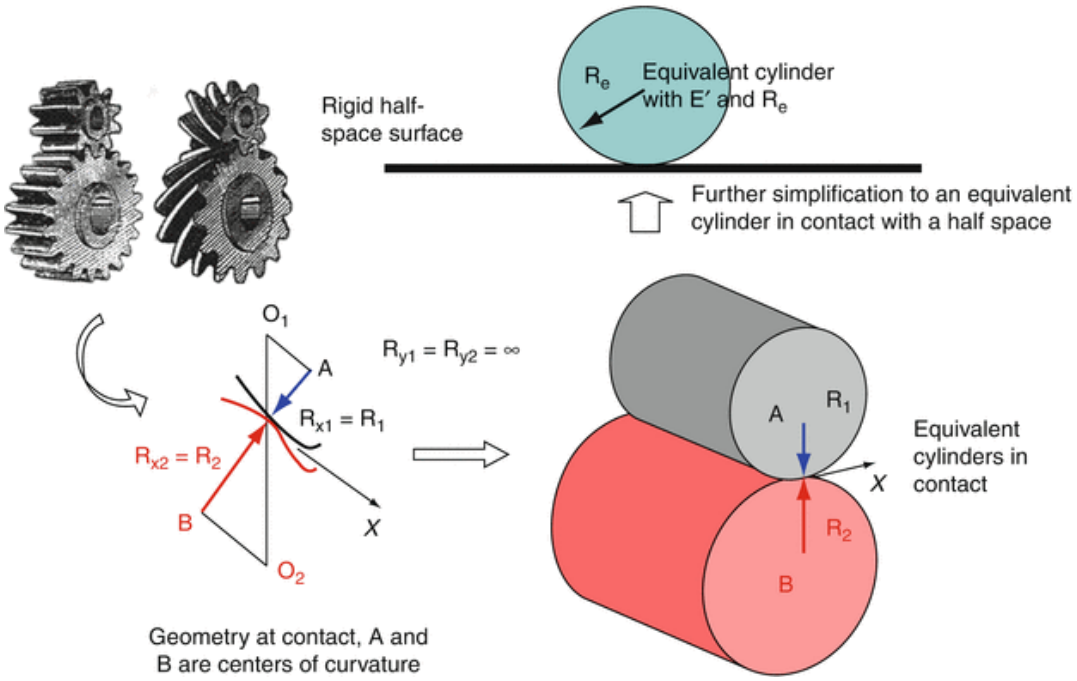

Figure 2.2: Line Contact Demonstration [14]

Assumptions in Line Contact Theory:

1. **Elastic Behaviour:** The materials in contact are assumed to behave purely elastically, meaning they deform reversibly under load. This assumption implies that there is no permanent deformation (plastic deformation) of the contacting bodies, and they return to their original shape once the load is removed.
2. **Smooth Surfaces:** The contacting surfaces are assumed to be perfectly smooth and free of defects or asperities. This assumption simplifies the analysis by neglecting the effects of surface roughness and irregularities. Surface roughness can affect the contact behaviour, but it is often considered separately in tribological studies.
3. **Symmetrical Loading:** The bodies are assumed to be loaded symmetrically along the line of contact. This ensures that the contact pressure distribution is symmetrical about the centre of the line. Symmetrical loading simplifies the mathematical analysis and allows for the prediction of a uniform pressure distribution along the line of contact.
4. **Linear Elasticity:** The materials are assumed to exhibit linear elastic behaviour, meaning that the relationship between stress and strain is linear within the elastic deformation range. This assumption simplifies the stress analysis by allowing the use of linear elasticity equations to relate the applied load to the resulting deformation and stress distribution.

5. **Small Deformation**: The deformation of the contacting bodies is assumed to be small compared to their dimensions. This assumption allows for the linearization of the elasticity equations and simplifies the analysis by neglecting higher-order deformation effects. It implies that the contact pressure and stress distribution remain within the elastic range of the materials.
6. **Uniform Material** Properties: The materials in contact are assumed to have uniform mechanical properties throughout their volume. This assumption simplifies the analysis by treating the materials as homogeneous and isotropic, meaning that their properties do not vary with position or direction. Material properties may vary due to factors such as composition, microstructure, and manufacturing processes.

2.4 ELLIPTICAL CONTACT (HERTZIAN THEORY) [14][15]

Hertzian elliptical contact take place between two bodies which are curved along both axes as shown in the figure and may be at arbitrary angles to one another. The case where both bodies have the same radius can be referred as either point or elliptical contacts. Any two surfaces which are curved along one axis and straight and parallel along the other can be converted into the contact of rigid curves against a flat half space. It typically refers to the contact of two surfaces that are curved or elliptical in shape. More it is seen in mechanical engineering in bearings and joints, where smooth and efficient motion transfer is required. This allows you to increase contact area compared to that of line contact which can distribute loads more evenly and reduce wear and stress on the surfaces involved.

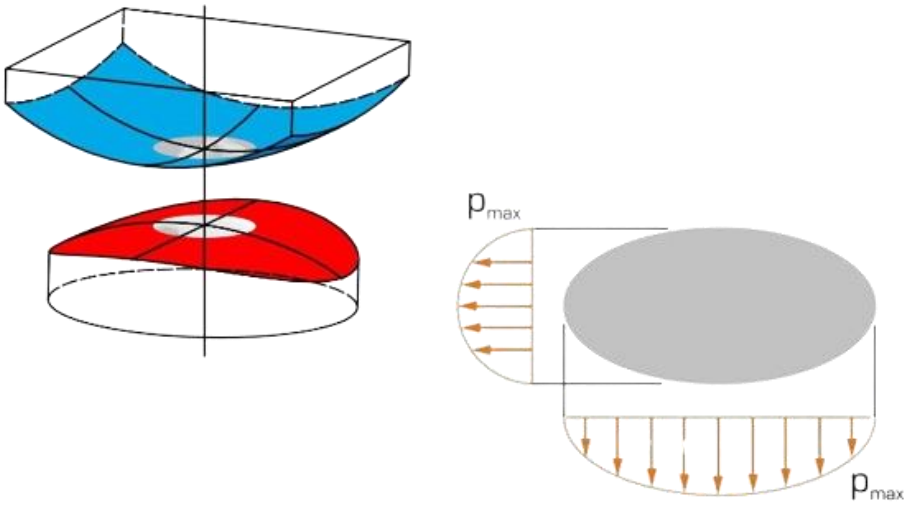

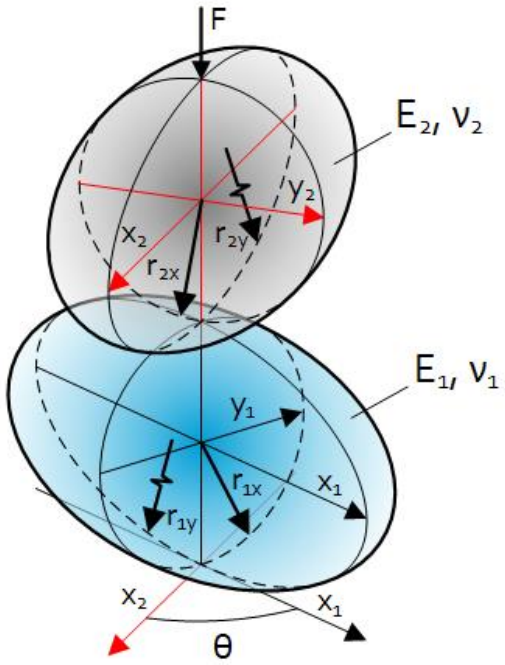

Figure 2.3: (a) Demonstration of Elliptical Contact (b) Pressure Distribution in Elliptical Contact [15]

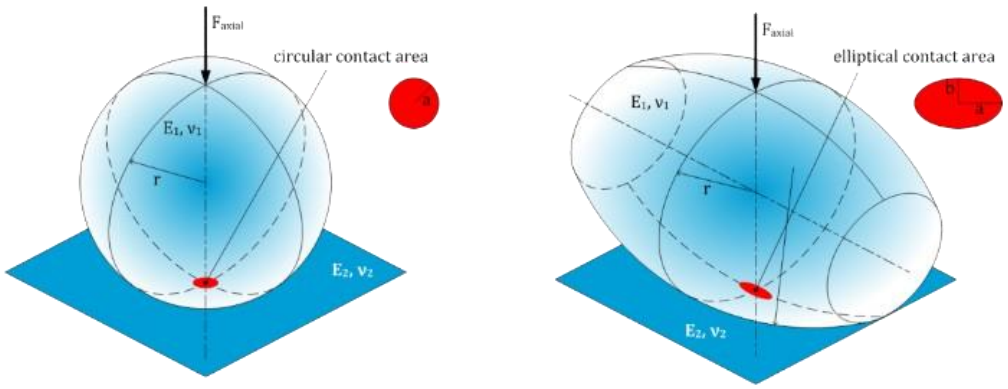

Figure 2.4: (a) Surfaces with the same radius on both axes will have a circular contact but (b) if there are different radii of both axes the contact will have an elliptical shape. [15]

In context of lubrication the shape of the contact area between two surfaces that are separated by lubricating film is elliptical in shape. The shape of contact can vary based on change in relative motion, load, and the properties of the lubricant. When the shape of contact resembles an ellipse, that may be due to factors like roughness, non-uniform loading or misalignment. This can lead to non-uniform distribution of pressure within the lubricated area, with the higher pressures concentrated near the edges of the ellipse. Elliptical contacts may experience mixed lubrication conditions, where both boundary lubrication (solid to solid contact with boundary

films) and hydrodynamic lubrication mechanism called Mixed Lubrication. Those require consideration of lubricant properties, surface roughness and operating conditions to ensure adequate protection against wear and friction.

Assumptions in Elliptical Contact Theory-

1. **Small Deformation:** The contact theory assumes that the deformations of the contacting bodies are relatively smaller to that of dimensions. This gives freedom to use linear elastic equations to determine the stress and deformation areas.
2. **Elliptical Shape of the Contact:** The contact area between the bodies is assumed to be elliptical in shape.
3. **No Slip at the Contact Interface:** It is assumed that there would be no slip conditions between the contacting surfaces, this simplifies the analysis but not hold true in all conditions, for example under the dynamic loading conditions.
4. **Homogeneous and Isotropic Materials:** The Mechanical properties of the bodies that are in contact are assumed to be homogeneous and Isotropic in nature. Also, the bodies are assumed to be rigid in the direction perpendicular to the contact interface, allowing deformation only within the contact plane.

2.5 FORMULATION [2]

This section contains all the governing equations and concepts used to develop the stochastic power loss model. For the power loss model, we had to first calculate the load, film thickness, contact pressure (hertzian), sliding velocity. These parameters are the inputs for the stochastic power loss model which calculates the effective viscosity of the lubricant which is then used to calculate the EHL friction coefficient. Presence of the system in mixed EHL regime mandates us to use the asperity contact friction and EHL friction parameters to compute the effective friction coefficient, which is then used to calculate the power loss of the system. The percent contribution of EHL friction and asperity contact is determined used the Greenwood Williamson model; which is a probabilistic model which adds the stochastic part to this power loss model. Greenwood Williamson uses set of Fourier series coefficients which if used in deterministic method would be computationally very expensive.

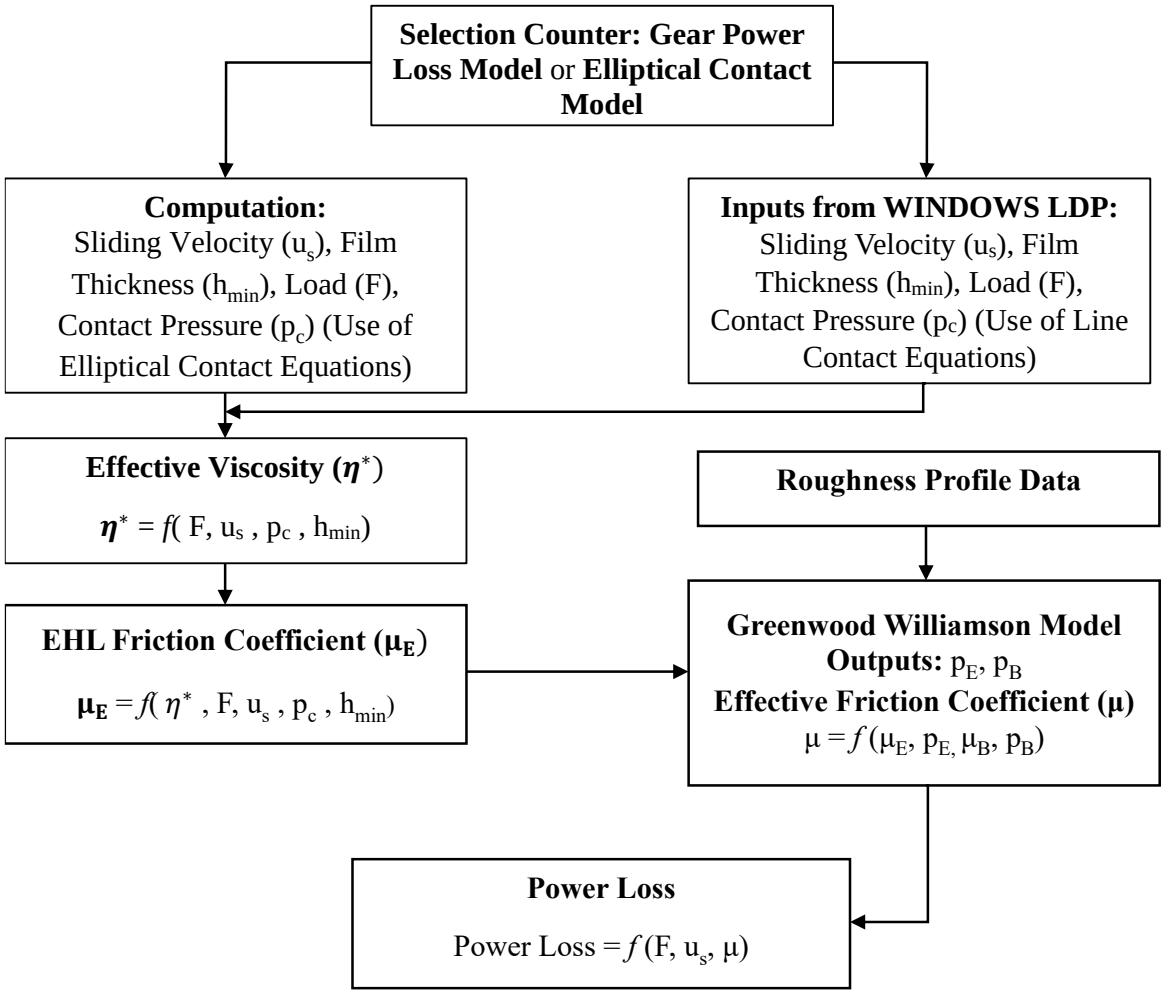

Figure 2.5: Stochastic Model computational flowchart

Table 2.1: Summary of Governing Equations [4][16]

Dowson and Toyoda formulation [8]	Minimum Film Thickness (h_{min}) for EHL line contacts	$h_{min}(\phi_1) = \frac{3.6G^{0.56}U^{0.69}(\phi_1)\rho'[\phi_1]}{w^{0.10}(\phi_1)}$ W = Load Parameter G = material parameter U = speed parameter $w(\emptyset 1) = \frac{F'(\emptyset 1)}{E'p'(\emptyset 1)}$ $G = \alpha E'$
Hertzian Pressure Distribution [9]	Maximum Contact pressure (p_c) of an elliptical pressure distribution	Pressure at any point over the fluid film is given by

		$P_{(x,y)} = P_c\left[1 - \left[\frac{r^2}{a^2}\right]\right]^{0.5}$
Ree-Eyring Fluid model [10]	For one dimensional line contact, hydrodynamic flow within contact flow is dictated by transient Reynolds equation. Effective viscosity (η^*) can be calculated	Shear stress: $\tau_m = \tau_0 \sin h^{-1}\left[\frac{\eta U_s}{\tau_0 h}\right]$ Reynolds Transient equation: $\partial[(f(\partial pc/\partial x)]/\partial x = \partial[ur\rho h_{min}]/\partial x + \partial[\rho h_{min}]/\partial t$
B.J. Hamrock and D. Dowson Formulation [16]	Minimum Film Thickness (h_{min}) for EHL Elliptical contacts of two rolling spheres or discs with crowning	$h_{min} = \frac{3.63G^{0.49}U^{0.68}(1 - e^{-0.68K})R}{w^{0.073}}$ W = Load Parameter G = material parameter U = speed parameter R = Effective radius K = Ellipticity ratio α = Pressure viscosity coeficient $w = \frac{F}{E'R^2}$ $G = \alpha E'$ $U = \frac{nu_r}{E'R}$ $K = \left(\frac{R_y}{R_x}\right)^{2/\pi}$
Hertzian Contact Pressure for Elliptical Contacts [18]	Maximum Contact pressure (p_c) of an elliptical pressure distribution for elliptical surfaces in contact	$P_C = \frac{3F}{2\pi C^2}$ $C = \left[AB\left(\frac{A+B}{2}\right)\right]^{\frac{-1}{3}}$ $A = \frac{1}{R_{rx}} + \frac{1}{R_{ry}}$ $B = \frac{1}{R_{dx}} + \frac{1}{R_{dy}}$

Disc Velocities [17]	Rolling and Sliding velocities between two discs at different velocities.	$u_r = \frac{u_2 + u_1}{2}$ $\quad u_s = u_2 - u_1$ u_1 = Velocity of roller u_2 = Velocity of disc
Tallian's Load Sharing Approach [3]	Tallian's Load sharing method gives equation to combine the losses due to asperity contact and fluid lubrication film.	$u = (u_E P_E) + (u_B P_B)$ $P_E + P_B = 1$ Power loss over one mesh cycle of gear: $\mathbf{P_L = \vec{u}.\vec{U}_s.F_m}$

2.6 DAWSON AND TOYODA FORMULATION – LINE CONTACT [8]

Elastohydrodynamic lubrication deals with the study of the interaction between elastic bodies in contact, such as rolling or sliding contacts like gears or bearings, and the lubricant present between them. The formulation presented by Dowson and Toyoda provides a means to calculate the central film thickness, which is a crucial parameter in EHL analysis. The central film thickness (h_{min}) represents the minimum oil film thickness within the contact region, and it is a vital factor in determining the efficiency, load carrying capacity, and lubrication performance of mechanical components operating under EHL conditions.

$$h_{min}(\phi_1) = \frac{3.6 \times G^{0.56} U^{0.69} (\phi_1) \rho'[\phi_1]}{w^{0.10}(\phi_1)} \quad \ldots Eq.(2.1)$$

$$w(\emptyset 1) = \frac{F'(\emptyset 1)}{E' p'(\emptyset 1)} \quad \ldots Eq.(2.2)$$

$$G = \alpha E' \quad \ldots Eq.(2.3)$$

α = Pressure Viscosity Coefficient

W = Load Parameter

G = material parameter

U = speed parameter

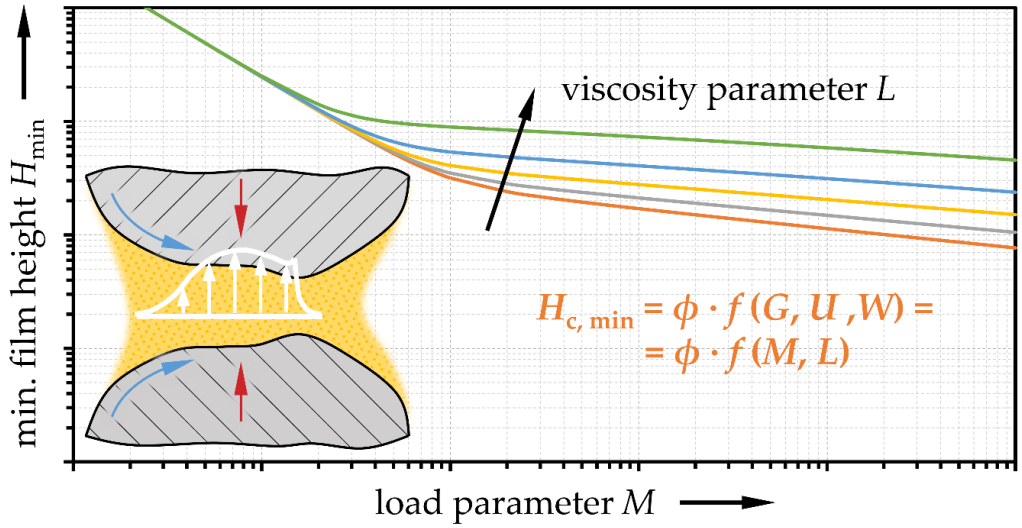

Figure 2.6: Distribution of Load due to fluid during Gear mesh [20]

In EHL, the lubricant film thickness varies across the contact region due to the deformation of the contacting bodies and the pressure distribution within the lubricant. The central film thickness represents the thinnest point within the contact, and it is a crucial parameter in determining the efficiency, load-carrying capacity, and lubrication performance of mechanical components operating under EHL conditions. The calculation and understanding of the central film thickness are essential in designing and optimizing high-performance mechanical systems to ensure proper lubrication and prevent excessive wear or failure of the components.

2.7 B.J. HAMROCK & D. DOWSON FORMULATION: ELLIPTICAL CONTACT [16]

The Hamrock and Dowson formulation builds upon the foundational research of Higginson (1979), which introduced sophisticated approximations for point or elliptical contact. This extended work provides equations for determining both the minimum and central film thickness in elastohydrodynamic elliptical contact scenarios. These equations are derived under the assumption of isothermal conditions and the Newtonian behaviour of the lubricant.

$$h_{min} = \frac{3.63G^{0.49}U^{0.68}(1-e^{-0.68K})R}{w^{0.073}} \qquad \dots Eq.\,(2.4)$$

$$w = \frac{F}{E'R^2} \quad \& \quad G = \alpha E' \qquad \dots Eq.\,(2.5)$$

$$U = \frac{nu_r}{E'R} \quad \& \quad K = \left(\frac{R_y}{R_x}\right)^{2/\pi} \qquad \dots Eq.\,(2.6)$$

W = Load Parameter

G = material parameter

$U = \text{speed parameter}$

$R = \text{Effective radius}$

$K = \text{Ellipticity ratio}$

$\alpha = \text{Pressure viscosity coefficient}$

Here, the well-known dimensionless constants U, G, and W were created to determine the impact of the practical variable's loadings, materials, and speed. The two contacting discs are shown in the figure 2.7. The principal radii of curvature with no deformation are R_{rx} , R_{dx} in X direction and R_{ry}, R_{dy} in Y direction. The principal radii of the equivalent ellipsoid at contact point are given by,

$$R_x = \left[\frac{1}{R_{rx}} + \frac{1}{R_{dx}}\right]^{-1} \quad R_y = \left[\frac{1}{R_{ry}} + \frac{1}{R_{dy}}\right]^{-1} \qquad \ldots Eq.(2.7)$$

And the effective radius is given by,

$$R = \left[\frac{1}{R_x} + \frac{1}{R_y}\right]^{-1} \qquad \ldots Eq.(2.8)$$

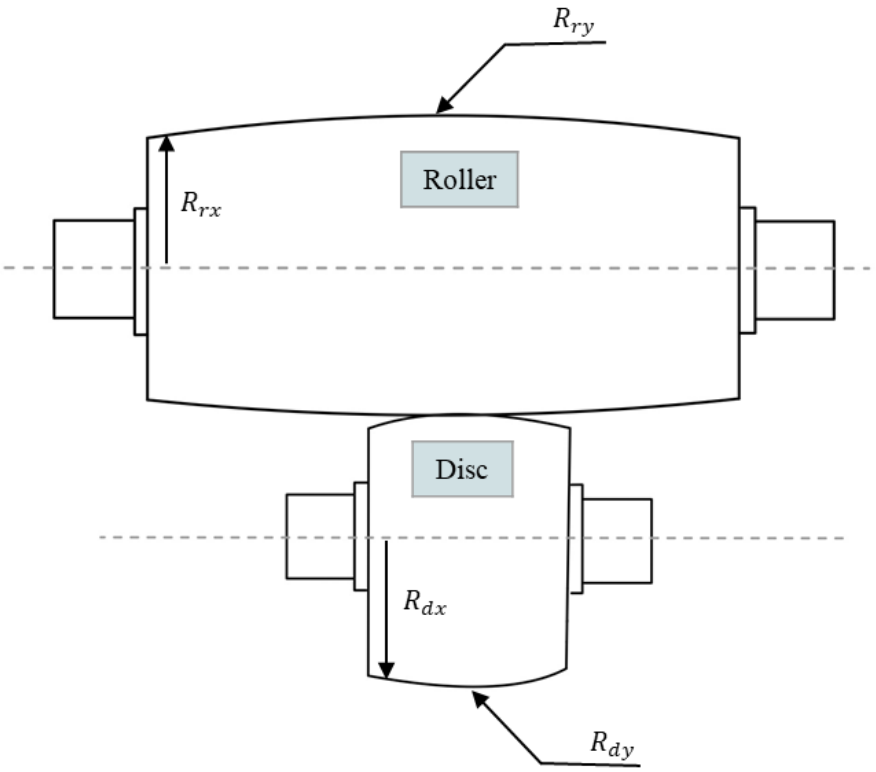

Figure 2.7: Disc Roller Elliptical contact schematic

2.8 HERTZIAN PRESSURE DISTRIBUTION [9][15]

Hertzian pressure distribution, also known as Hertz contact stress or Hertzian contact theory, describes the pressure distribution between two elastic bodies in contact under a given load. Hertzian pressure distribution is primarily applied to the analysis of contact between two smooth, spherical, or cylindrical bodies. It assumes that both contacting bodies are perfectly elastic and have a high level of symmetry. The theory is commonly used in various engineering applications, such as ball bearings, gears, and rolling element bearings. The Hertzian pressure distribution predicts that the pressure between the contacting surfaces is highest at the centre of the contact region and gradually decreases towards the periphery. The pressure distribution follows a parabolic pattern for spherical contacts and an elliptical pattern for cylindrical contacts.

Assumptions:

- Surface are infinitely large half-spaces.
- Pressure profile is parabolic (which assumes that the shape of the bodies in contact can also be approximated well with parabolic shapes, e.g., sphere, ellipse, or a cylinder)
- All the assumptions of the classical theory of elasticity apply.

For Line contact, pressure at any point over the fluid film is given by

$$P_{(x,y)} = P_c \left[1 - \left[\frac{r^2}{a^2}\right]\right]^{0.5} \quad \ldots Eq.\ (2.9)$$

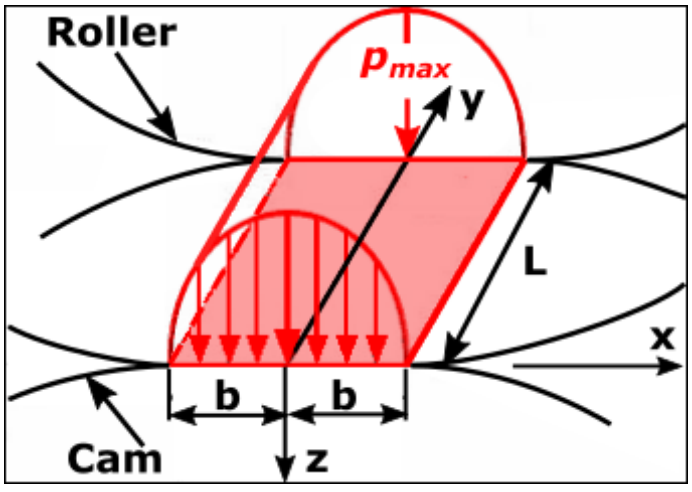

Figure 2.8: Pressure profile in a Hertzian line contact [15]

For Elliptical contact, maximum pressure is given by

$$P_C = \frac{3F}{2\pi C^2} \qquad \ldots Eq.(2.10)$$

$$C = \left[AB\left(\frac{A+B}{2}\right)\right]^{\frac{-1}{3}} \qquad \ldots Eq.(2.11)$$

$$A = \frac{1}{R_{rx}} + \frac{1}{R_{ry}} \quad \& \quad B = \frac{1}{R_{dx}} + \frac{1}{R_{dy}} \qquad \ldots Eq.(2.12)$$

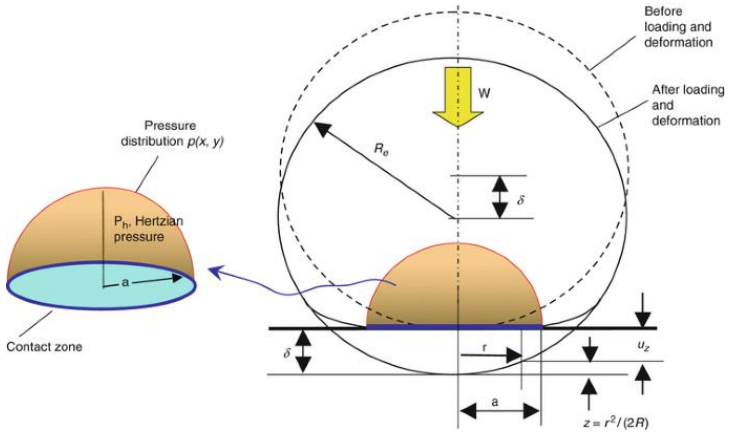

Figure 2.9: Pressure profile in a Hertzian elliptical contact [15]

2.9 REE EYRING FLUID MODEL [10]

The Eyring fluid model assumes that the flow of the fluid is governed by the presence of activated particles or entities within the fluid that need to overcome an energy barrier to move. The model is often used to describe the behaviour of fluids with a yield stress, meaning they require a certain force to start flowing. These fluids behave as a solid until the applied stress exceeds the yield stress, at which point they flow like a viscous fluid.

The shear stress (τ) in the Eyring fluid model is given by the following equation:

$$\boldsymbol{\tau} = \boldsymbol{\tau_y} + (\boldsymbol{\eta\gamma}) \qquad \ldots Eq.(2.13)$$

$\boldsymbol{\tau}$ is the total shear stress.

$\boldsymbol{\tau_y}$ is the yield stress, which represents the minimum stress required to initiate flow.

η is the consistency index, a measure of the fluid's resistance to flow.

$\boldsymbol{\gamma}$ is the shear rate, which is the velocity gradient between adjacent fluid layers.

The Eyring fluid model assumes a linear relationship between the shear stress and the shear rate, making it a relatively simple rheological model. However, it may not accurately describe all types of non-Newtonian fluids, especially those with more complex flow behaviours such as shear-thinning or shear-thickening. For fluids that exhibit such behaviours, more

sophisticated rheological models like the Ree-Eyring model or the power-law model may be used. Eyring fluid model is used to describe the flow behaviour of non-Newtonian fluids under Couette flow conditions.

2.10 TALLIAN'S LOAD SHARING APPROACH [3]

The concept of partial elastohydrodynamic (EHD) Hertzian contacts is defined between solids with real (rough) surfaces, using the film thickness/RMS roughness ratio h/σ as parameter. The influence of the partial EHD condition is described on EHD film thickness, normal load sharing between asperities and EHD film, frictional traction, mild and severe wear, surface fatigue and spalling fatigue. Kinematic effects of the traction vs. sliding rate relationship characteristic of partial EHD are identified in rolling bearings. Rough surfaces are treated as two-dimensional random processes, using height, slope, curvature, and level-crossing statistics derived, for Gaussian height distributions, with the aid of statistics of the height and its first two derivatives. Scanning electron microscope observations of surfaces are used to visualize asperity geometry, lay, and defect population. Normal load and traction force sharing between EHD film and asperities is analysed for plastic and elastic asperities. Indentation hardness and h/σ are parameters of plastic load sharing. Elastic load sharing depends on elastic modulus, h/σ, and asperity slope and may depend weakly on the spectral distribution of asperity amplitudes. Traction force sharing depends on similar parameters and on the EHD traction/ sliding rate function. Stresses in elastic asperities and the size of asperity contact areas are expressed in terms of roughness height, its derivatives and h/σ. Roughness parameters influencing wear, smearing (galling), and surface fatigue are identified from the asperity contact stresses obtained.

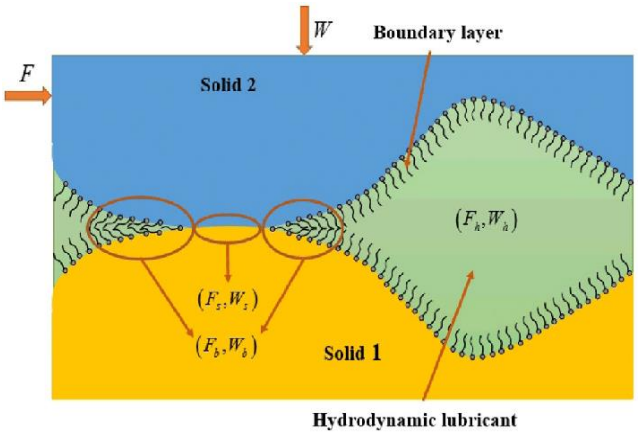

Figure 2.10: Mixed EHL Lubrication Regime [21]

In mixed EHL regime, the effective friction coefficient of the system is sum of friction due to the lubrication oil (EHL friction coefficient) and friction due to asperity (contact friction coefficient). This load sharing approach uses a formulation that implements the use of Greenwood Williamson Model and is given by:

$$u = (u_E P_E) + (u_B P_B) \quad \ldots Eq.(2.14)$$

$$P_E + P_B = 1$$

2.11 GREENWOOD WILLIAMSON MODEL [2]

According to the Greenwood Williamson theory, a nominally flat surface will be covered with a distribution of asperities, with a density per unit area, all the same size except that their heights follow a statistical distribution with a standard deviation, and spherical, at least near their summits. Greenwood Williamson roughness contact model implements the use of Fourier series coefficients to calculate the root mean square roughness and average roughness of the gear surface. The surface roughness data is fed into the model using a profilometer that outputs the data in .MOD format. The Greenwood Williamson roughness contact model addresses the elastic contact between two surfaces.

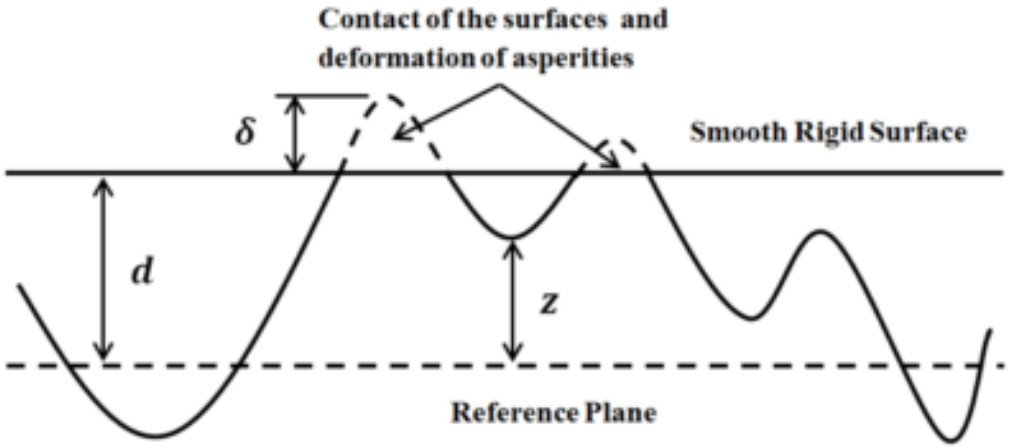

Figure 2.11: Contact Between Smooth and Rough surface showing elastic deformation [4]

The Greenwood Williamson model calculates the statistical probability of an asperity to be in contact using a comparison of a single normally rough surface with a perfectly smooth surface. Using 0th, 2nd and 4th order Fourier series coefficients, equivalent roughness profiles are determined and subsequently asperity density(n), asperity summits radii (β), summit height variance (σ_s) can be calculated using McCool's parameterization method.

$m_0 = AVG[(R^p)^2] + AVG[(R^g)^2]$

$m_2 = AVG[(dR^p/d\phi)^2] + AVG[(dR^g/d\phi)^2]$

$m_4 = AVG[(d^2R^p/d\phi^2)^2] + AVG[(d^2R^g/d\phi^2)^2]$ $\ldots Eq.(2.15)$

$$d = \left[\left(\frac{h_{min}}{R_q}\right) - \left(\frac{4}{\pi a}\right)^{0.5}\right] \quad \ldots Eq.(2.16)$$

$$\sigma_s = \left(\frac{1-0.8968}{\alpha}\right)^{0.5} m_0^{0.5} \quad \ldots Eq.(2.17)$$

$$\alpha = \frac{m_0 m_4}{m_2} \quad \ldots Eq.(2.18)$$

$$n = \frac{m_4}{32.42 m_2} \quad \ldots Eq.(2.19)$$

$$\beta = 0.375\left(\frac{\pi}{m_4}\right)^{0.5} \quad \ldots Eq.(2.20)$$

Asperity Contact Area $A = \pi n \beta \sigma_s \int \left(x - \left(\frac{d}{\sigma s}\right) + wp\right) \phi(x)\, dx$ $\ldots Eq.(2.21)$

w_p = Distance of points in overlapping region

m_0 = 0th Fourier coefficient

m_2 = 2nd Fourier coefficient

m_4 = 4th Fourier coefficient

Asperity contact area (A) represents the term P_B which is used in the Tallian's Load Sharing Approach.

2.12 TEST SETUP FOR GEARS [5]

The high-speed gear efficiency test machine used in this study was designed by Moorhead during the spur gear efficiency phase of this project. Details of the test machine and the data acquisition and processing system are available in references. Figure 2.12 shows the schematic representation of test setup used to calculate power loss. The test machine used by Moorhead used to for gear efficiency testing basically calculates the mechanical power losses of the system and then subtracts the rolling losses i.e., bearing losses calculated using Palmgren formulation, Sliding Losses = Mechanical Losses – Rolling Losses

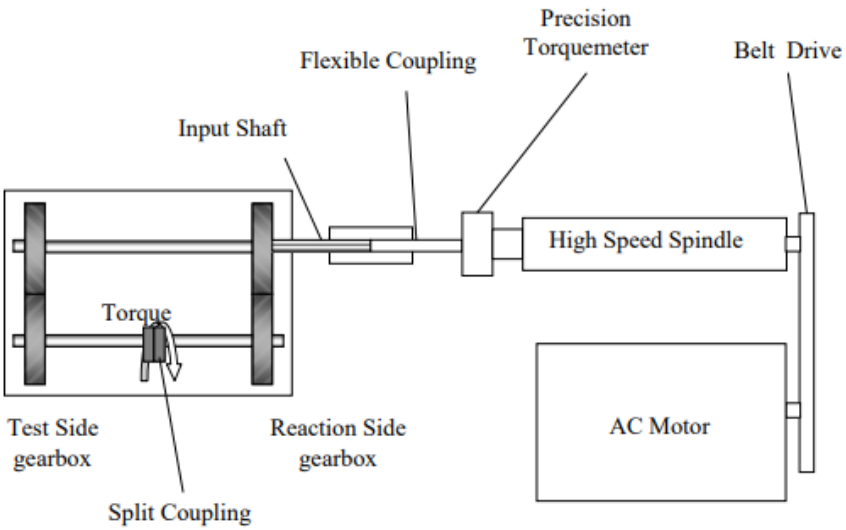

Figure 2.12: Schematic representation of test setup used for gears [5]

The machine consists of a pair of opposing, identical gear boxes, each containing a pair of unity-ratio helical (or spur) gears supported by rigid shafts mounted on two pairs of bearings. They are labelled as 'Test Gearbox' and 'Reaction Gearbox' in figure 2.12 for the purpose of distinguishing them while they are identical in every aspect. The assembly procedure for gears is the same as the one used in earlier spur gear efficiency tests and is described in greater detail in *reference* [5]. Each gear is held in place between two bearings, a deep-groove ball bearing on the outside (SKF Model 6206) and a four-point angular contact ball bearing (SKF Model QJ 206 MA) on the inside. The deep-groove ball bearing is not axially loaded (allowed to float axially), allowing all the axial load to be carried by the four-point angular contact ball bearing. In this arrangement, the bearings are not required to be preloaded. This avoids repeatability problems associated with setting the correct amount of preload for each test as well as changes in preload due to temperature effects that would be detrimental to the fidelity of the measurements. In figure 2.12, two gear pairs are connected to each other through flexible shafts. A split coupling is mounted on one of the shafts connecting the gearboxes and is used to apply a constant torque Tc to the closed loop [5]. The gearboxes are powered by a variable speed AC motor connected to a high-speed spindle. The connection is through a 3:1 ratio belt drive. The high-speed spindle is connected to the splined input shaft of the reaction gearbox through a flexible coupling. The gearboxes and shafts connecting them are mounted on a sliding table, allowing easy engagement and disengagement of the splined input shaft from the coupling. The torque loss in the system TL is measured 12 using a high precision, non-contact type torque-meter (Lebow model TMS 9000) that is mounted between the high-speed spindle

and the input shaft to the reaction gearbox. The temperature control is achieved through the lubrication system that supplies the lubricant to the gear meshes and bearings through nozzles. The oil temperature is measured at various points (in the lubricant heating unit, and the supply and return points) on the test machine, which is then used to control the lubricant temperature to a preset value. The lubrication systems and parameters of the test and reaction gearboxes are kept identical to ensure the same thermal conditions for both gearboxes. Likewise, oil flow rates are tightly controlled and monitored as well. The maximum operating speed that the test machine can reach is 10,000 rpm.

Table 2.2: Speed and Torque conditions with each torque values iterated over the 3 values of speed

Speed Conditions (RPM)	**Torque (Nm)**
2000	140
4000	239
6000	413
	546

The surface roughness profiles of each test gear in the involute direction were also measured by using a Taylor-Hobson Form Talysurf-120 surface profiler with the aid of a special gear mounting fixture. In addition, run-in average centreline roughness R_a and the root-mean-square roughness R_q values for all nine test gear pairs are listed in Table 3.

Table 2.3: Gear Roughness Data for Helical Gears

Gear	**R_a - Average (um)**	**R_q - RMS (um)**	**Used RMS (um)**
A	0.28	0.37	0.371
B	0.22	0.28	0.252
C	0.24	0.32	0.371
D	0.21	0.28	0.252

E	0.23	0.29	0.252
F	0.31	0.39	0.371
G	0.21	0.27	0.252
H	0.26	0.34	0.371
I	0.26	0.34	0.371

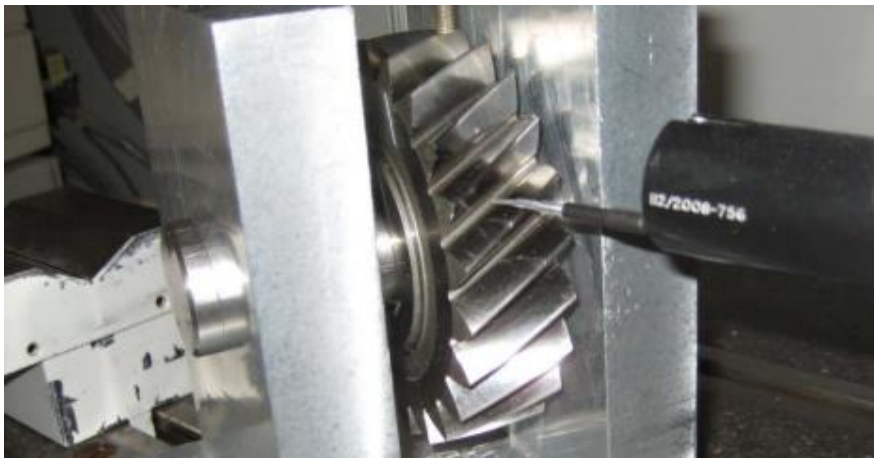

Figure 2.13: Measurement of surface roughness using the Taylor-Hobson Form Talysurf-120 surface profiler with the aid of a OBJ special mounting fixture. [5]

Referring to the assumptions, used RMS value in the Stochastic model is different because of the unavailability of the data concerned with the roughness traces of gear surface. Hence. Roughness profiles having nearest RMS values were used to compute the power loss values.

2.13 TEST PROCEDURE AND GEAR PARAMETERS [4]

Majorly two master's theses were used to obtain the gear dataset and the measured power loss to validate the stochastic model.

A] Anashanshley's Thesis (Spur Gears) [4]

From the previous research done on the stochastic model, a basic code that was brute forced for a single dataset was developed to verify the working of the model. However, this was not enough as to make the model useful, it had to be generalized to an extent where it is applicable for any of the gear dataset and torque and speed values. Modifications were made to the existing set of code so that it becomes generalized with required user inputs and roughness profile data

and the model was working fine. One of the major issues was getting the inputs of roughness profiles Talysurf profilometer provides roughness profiles in .MOD format which outputs x axis data in first of the data and y axis in the second half. Data from those .MOD files was acquired and then stored in separate files for x and y data respectively. For this part, we had used a different set of data from the helical gear data set to verify the values. This data was acquired from the Anashanshley's thesis [4].

Table 2.4: Speed and Torque conditions with each torque values iterated over the 5 values of speed

Speed Conditions (RPM)	**Torque (Nm)**
500	0
1000	50
1500	100
2000	150
2500	

Gear roughness pairings used based on the type of surface finish are:

0.05 – 0.05: ISF - ISF

0.14 – 0.08: Super honed - Super honed

0.48 – 0.05: Ground - ISF

0.46 – 0.47: Ground - Ground

These values signify the RMS values of surface roughness of gears and these values in um.

B] Vaidynathan's Thesis (Helical Gears) [5]

All the tests in this study were conducted by using a typical automatic transmission fluid (ATF) as the lubricant, provided at a fixed temperature of 90°C. A LabVIEW interface is used to monitor the temperature as well as set the test duration and rotational speed. A calibrated jet lubrication system was used to deliver controlled amounts of oil to gear meshes and bearings, like the one used in the spur gear studies conducted previously [5]. The new test gears were first run-in at a low torque (140 Tc = Nm) and speed (**Ω** = 2000 rpm) values for a duration of one hour. Similarly, it was performed for another 4 values of torque and 3 values of speed in an iterative manner. The actual duration of each test was kept at 11 minutes [5]. The torque

measured by the torque-meter was the total torque provided to the closed loop by the motor to maintain operation, and represented the torque loss of the entire closed loop. After completion of the test, any electronic drift of the torque-meter was recorded, to be subtracted from the torque loss value obtained. Prior to conducting the experiments, the lubrication system was set at the testing temperature. The system was allowed to stabilize for an hour before testing. Prior to each test, it was ensured that the lubricant levels in the lube sump were above the minimum required levels for a complete sequence of tests.

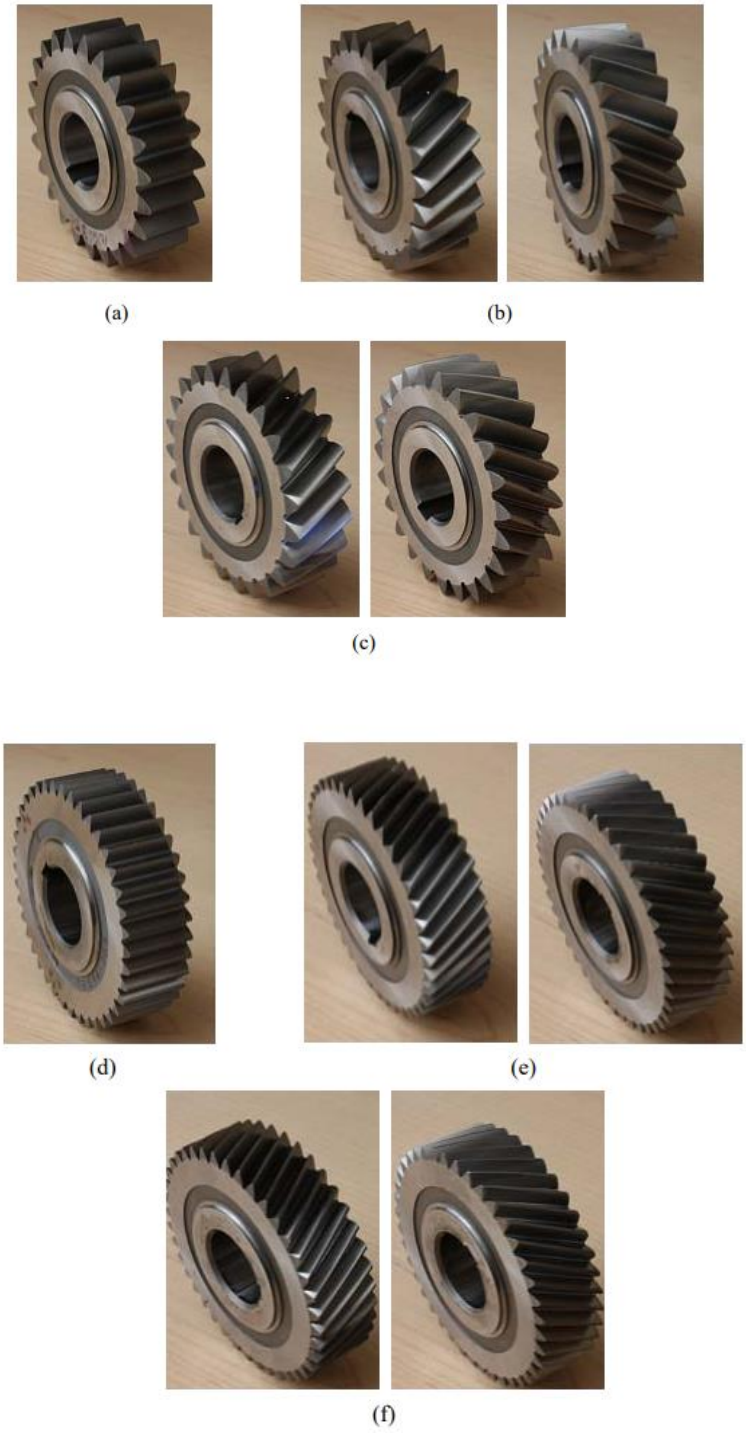

(a) (b) (c) (d) (e) (f)

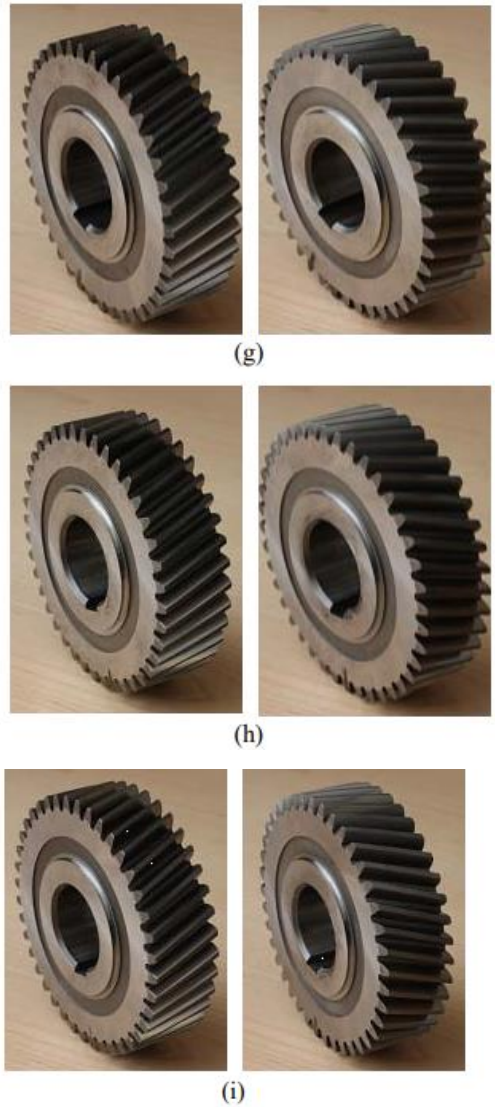

Figure 2.14: Pictures of the gear test specimens used in the study; (a) gear set A, (b) gear set B, (c) gear set C, (d) gear set D, (e) gear set E, (f) gear set F, (g) gear set G, (h) gear set H, and (i) gear set I [5]

Table 2.5: Gear Parameters (All dimensions are in mm unless specified)

Parameter	**A**	**B**	**C**	**D**	**E**
Number of Teeth [Z]	23	23	23	40	40
Normal Module	3.95	3.45	3.42	2.32	1.98
Normal Pressure Angle [deg.]	25	25.9	22.7	26.5	26.5
Helix Angle [deg.]	0	30	30	0	30

Base Diameter	82.34	79.85	82.34	81.89	79.30
Major Diameter	100.25	100.25	100.25	95.88	95.88
Minor Diameter	81.36	81.36	81.23	85.72	85.72
Tooth thickness	6.43	6.16	6.422	2.92	3.51
(Transverse) Backlash	0.195	0.125	0.129	0.189	0.121
Tip Relief	0.07	–	–	0.07	–
Tip Relief start [deg.]	36.0	–	–	32.5	–
Lead Crown	0.008	0.006	0.006	0.008	0.006

Parameter	**F**	**G**	**H**	**I**
Number of Teeth [Z]	40	40	40	40
Normal Module	2.01	2.18	2.15	2.14
Normal Pressure Angle [deg.]	23.40	20.22	17.75	16.55
Helix Angle [deg.]	30.00	17.5	20.00	21.00
Base Diameter	81.89	85.36	86.61	87.19
Major Diameter	95.88	95.95	95.95	95.88
Minor Diameter	85.72	85.70	85.34	85.22
Tooth thickness	2.91	3.51	3.51	3.51
(Transverse) Backlash	0.125	0.121	0.123	0.124
Tip Relief	–	–	–	–
Tip Relief start [deg.]	–	–	–	–
Lead Crown	0.006	0.006	0.006	0.006

2.14 ELLIPTICAL CONTACT MODEL EXPERIMENTAL SETUP [17]

For the Elliptical contact model's experimental setup, the friction coefficient, wear, and scuffing performance of roller specimens produced from two different gear steels were assessed using a two-disk test machine, as is explained in S. Shon's thesis. With the help of this test apparatus, two disks can be pushed up against one another and run at specific rolling and sliding speeds. The larger of the two disk specimens, the disk, and the smaller roller were individually controlled to rotate at different speeds to reach the desired speed conditions. Figure 2.15 below shows the drive units that powered the roller and the disk which were 10 HP, 3-phase AC vector motors coupled to a 2:1 ratio timing belt.

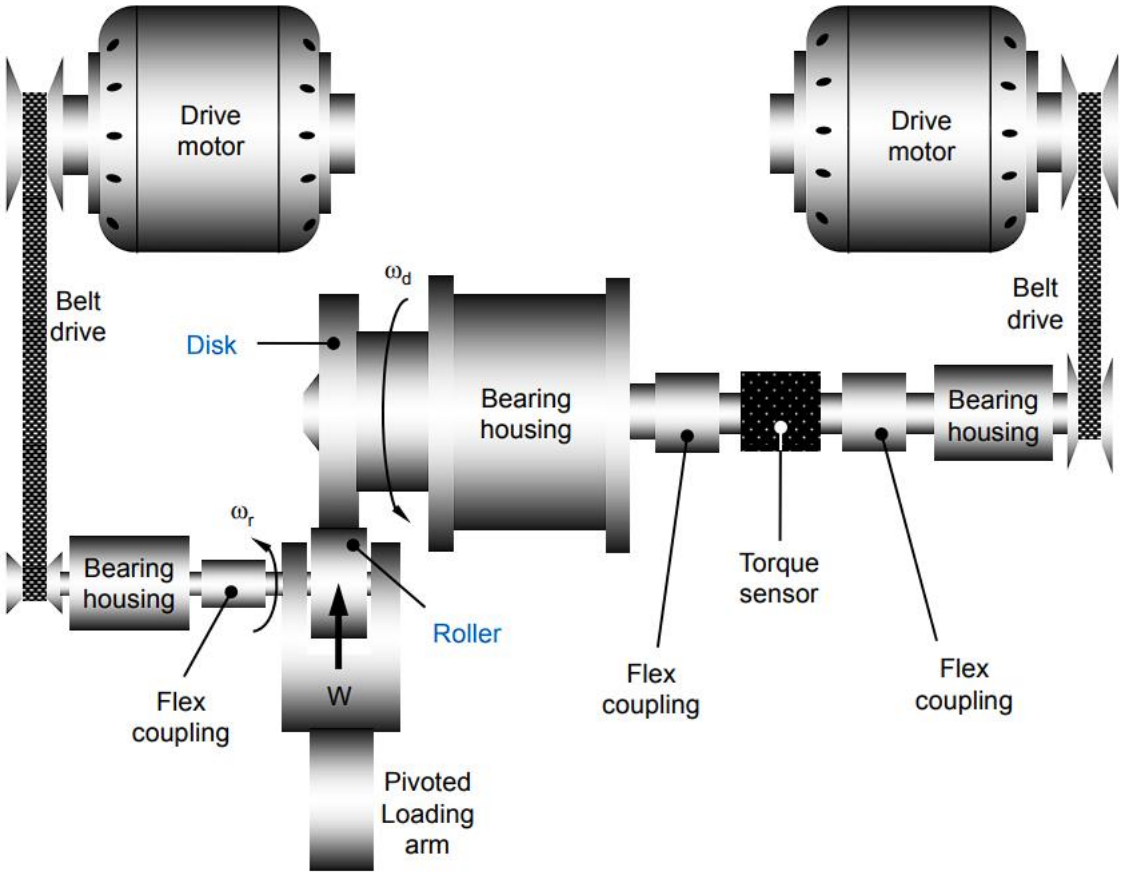

Figure 2.15: Schematic of the two-disk test machine used in this study [17]

Two rolling element bearings in their housing provided stiff support for the disk-side drive shaft. One needle roller bearing and two very precise ball bearings supported the roller shaft in the loading fixture on opposite sides. To axially secure the roller's position, the roller shaft was threaded on one side to accommodate a washer and locking nut. When the roller was in

nominal unloaded condition, it was not in contact with the disk but extremely close. The loading lever pushed the roller and its shaft towards the disk to bring the two in contact, in the process, offsetting the roller shaft axis from the roller-side drive shaft. The loading lever can be seen in figure 2.16 below.

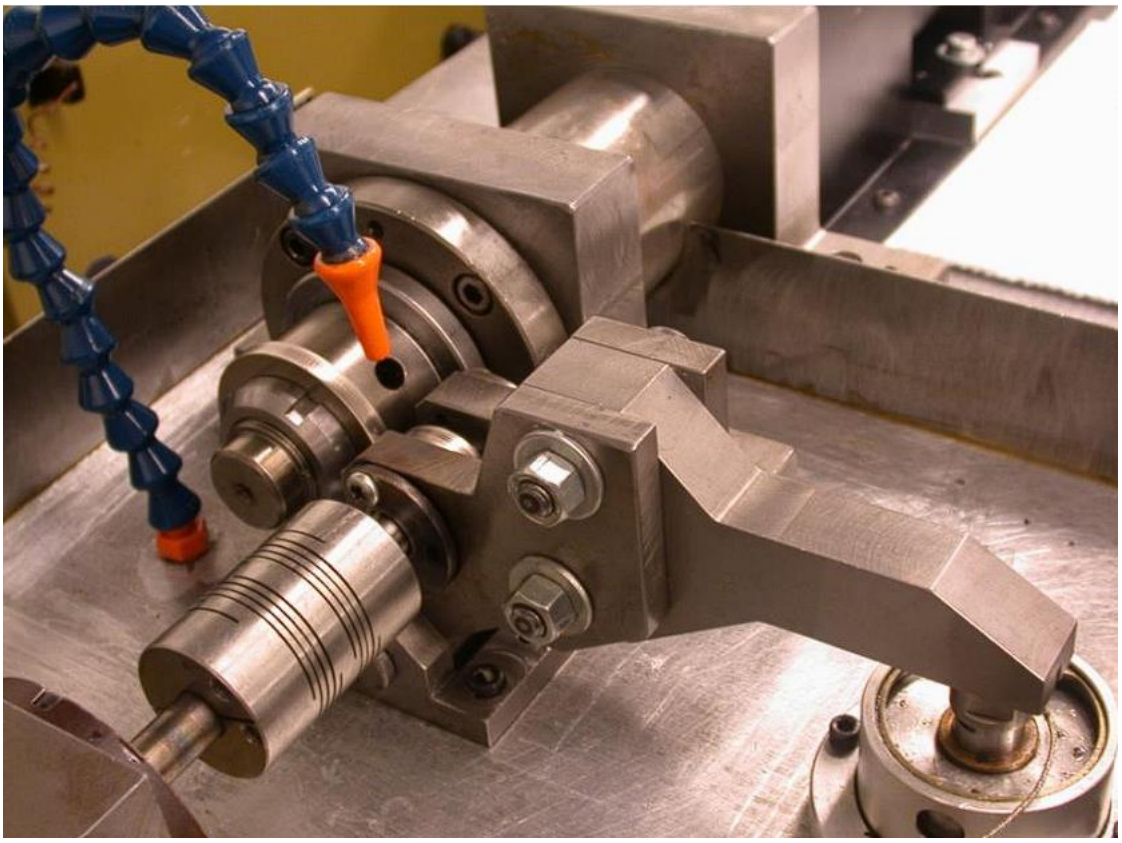

Figure 2.16: Close up view of the test pair, roller and disk shafts, roller-side flexible coupling and the loading arm mechanism. [17]

As seen in Figure Y, a flex-coupling (helical spring type) was utilized to connect the roller shaft to the roller-side drive shaft to account for this misalignment during loading. To stop axial motion, the disk was shrunk fit onto the shaft and a locking nut was tightened. This shaft was supported tightly by a needle thrust bearing and four angular contact ball bearings. During the experiment, a compact, low-flow lubricating system was employed. After being heated inside the reservoir, the oil was pushed into the test area via flexible hose. The oil could only reach a maximum temperature of 150˚C. Within the range of 0.4 to 3.3 lpm, any constant flow rate was feasible. Restricting specific hose portions and adjusting the nozzle allowed for the achievement of far lower flow rates—less than 0.1 lpm. Through a regulated proportional valve that connected to a pneumatic cylinder, the loading arm applied a normal force. A standard load of 4,450 N, corresponding to a pressure of up to 550 kPa, was supplied to the cylinder. A

button head-type load cell with a 1,112 N threshold was used to monitor this force. It was placed in a little recess at the end of the loading arm. Two flexible couplings in the form of helical styles were used to connect the disk shaft and motor of the torque-meter, which had a 3.5 Nm capacity. A LabVIEW program was used to control the drives and also monitor parameters such as torque and temperatures with the help of the associated measuring devices providing the necessary inputs.

2.15 DISC AND ROLLER PARAMETERS [17]

The two specimens used in the experiment, disk and roller, were made of material AISI 5120. As is illustrated in Shon's paper outlining the experimentation, and in Figures 2.17 and 2.18 below, which show the engineering drawings for roller and disk specimens respectively, the roller had an outside radius of 15.875 mm, with no lead crown and a face width of 7.6mm. Subsequently, the disk had a radius of 28.575 mm and a face width of 6.3mm. The disk also possessed crowing of a magnitude of 75 mm. The crowning served to provide an elliptical contact pattern and ensure no edge loading. The surface finish on both, the disk and the roller were of magnitude 0.43μm. The lubrication provided to the specimens of 80W90 and MILPRF 23699 was selected keeping in mind traditional steel gear applications. The viscosity of the MIL-PRF-23699 at 100˚C is typically 5.25 mm^2/s, where the viscosity of the 80W90 at the same condition is 14.2 mm2/s. The test parameters saw the use of rolling speeds of 5m/s and 15m/s.

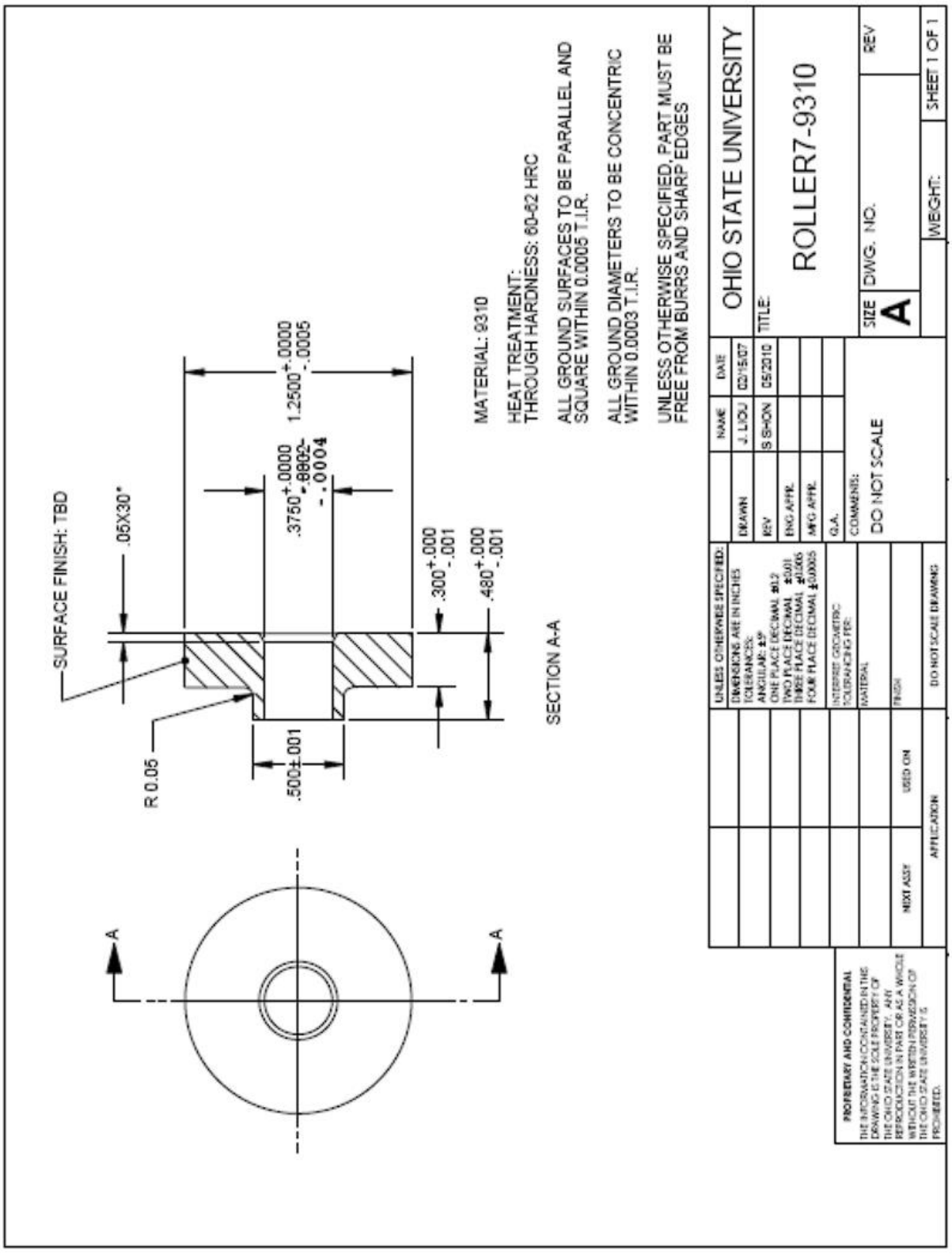

Figure 2.17: Engineering drawing of the roller specimen. [17]

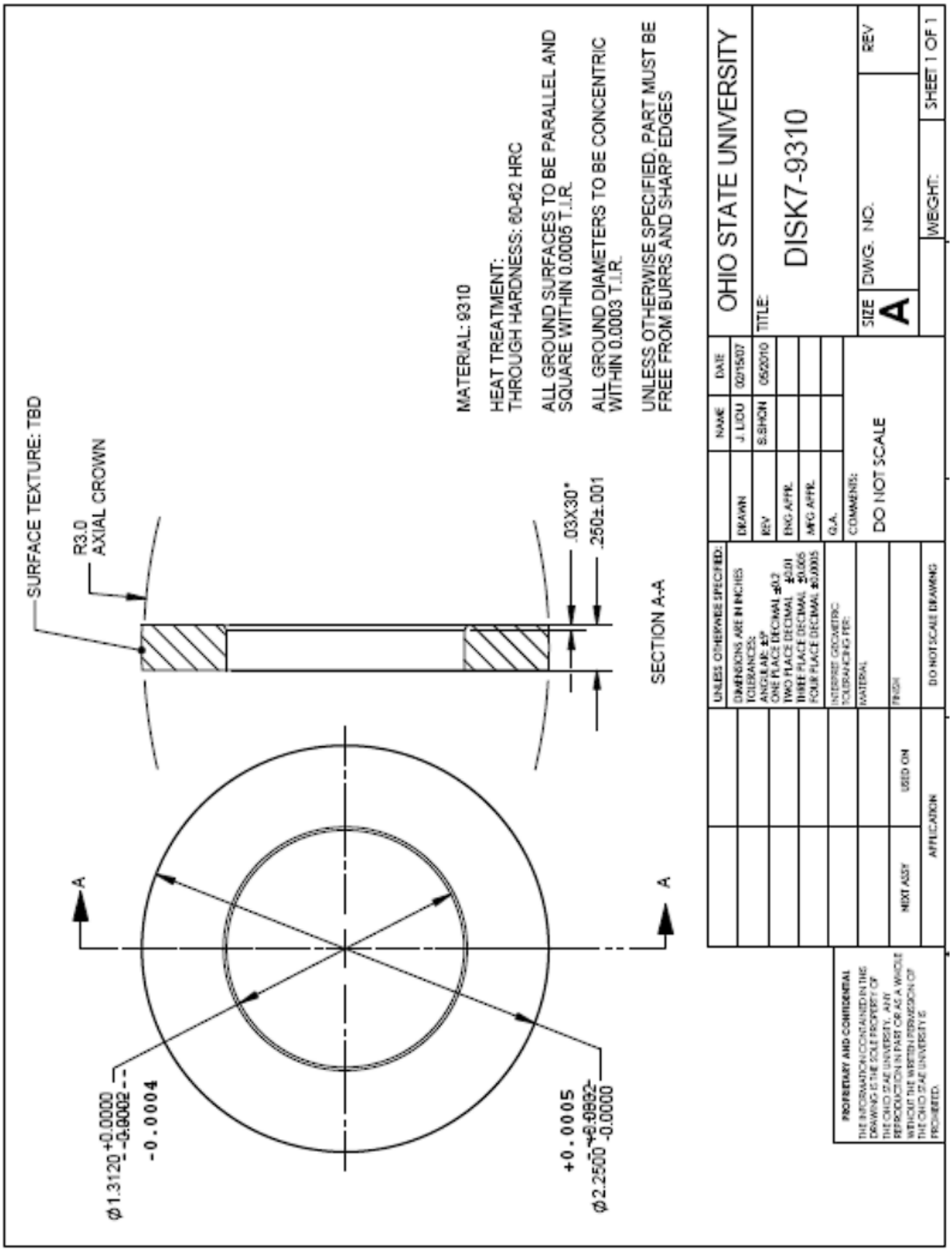

Figure 2.18: Engineering drawing of the disk specimen. [17]

2.16 LITERATURE REVIEW SUMMARY

A novel model has been developed to predict the coefficient of friction in machine components operating under mixed lubrication regimes, a critical factor in designing energy-efficient power transmission systems. This model incorporates established theories on various friction mechanisms and their dependence on surface roughness. Notably, the model extends its applicability beyond gears (spur and helical) to encompass elliptical contacts, providing a versatile tool for a wider range of machine design problems. The validation process leverages experimental data from both gear and elliptical contact scenarios, solidifying the model's accuracy and effectiveness.

CHAPTER THREE: MODEL DEVELOPMENT

The line contact power loss model is used to calculate the mesh losses (sliding losses) in gears. The mechanical power loss in gears comprise of rolling losses and sliding losses. Rolling losses are contributed by bearings majorly and are load dependent losses whereas sliding losses are independent of load on the system. To validate the power loss model, an experimental test setup was used to determine power losses, which are recorded in the measured power loss database.

3.1 3D STOCHASTIC MODEL

The Stochastic power loss model is summation of power loss at each contact point on the gear tooth contact region. Initial model developed according to the Anashanshley's thesis [4] can be referred as the 2D stochastic model that would only consider time and the points on the centre of the face width along the Line of Action. This approach worked for the spur gears as the nature of contact in spur gears is symmetric. However, in helical gears due to the presence of the helix angle, the Line of Action is not parallel to the edge of the gear tooth so the 2D approach in stochastic model does not yield good results. The 3D stochastic model focused on the all the contact points that occurred in the gear tooth contact region formed by active face width and Line of Action that consisted of 2 dimensions and third dimension is time. Time is important dimension here to control the ability of model to discretize the gear tooth contact region. Timestep is a parameter that controlled the distance advanced along the Line of Action in unit time. More number of timesteps resulted in greater accuracy but computation load also increased.

$$\textbf{Power loss} = \frac{\sum_{1}^{i} \textbf{Force}.\textbf{Sliding Velocity}.\textbf{Friction Coefficient}}{\textbf{NPOS}} \qquad \dots Eq.(3.1)$$

i = Total number of contact points

NPOS = Total number of timesteps within each gear mesh period

The hatched region in figure 3.1 and figure 3.2 shows the gear tooth contact regions during the entire mesh cycle. Solid line in figure 3.1 represents a single row of points along face width. The thickness of the line is exaggerated for representation.

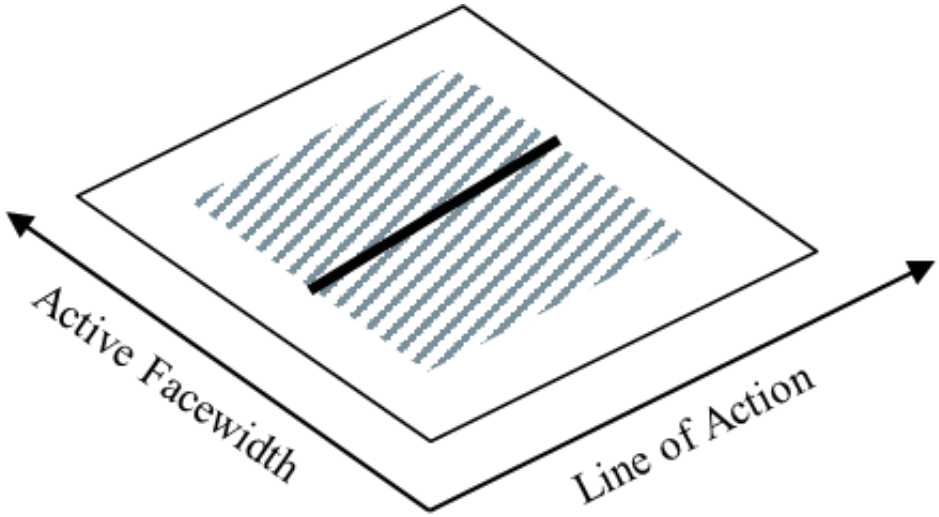

Figure 3.1: 2D Stochastic Model – only along the line of Action

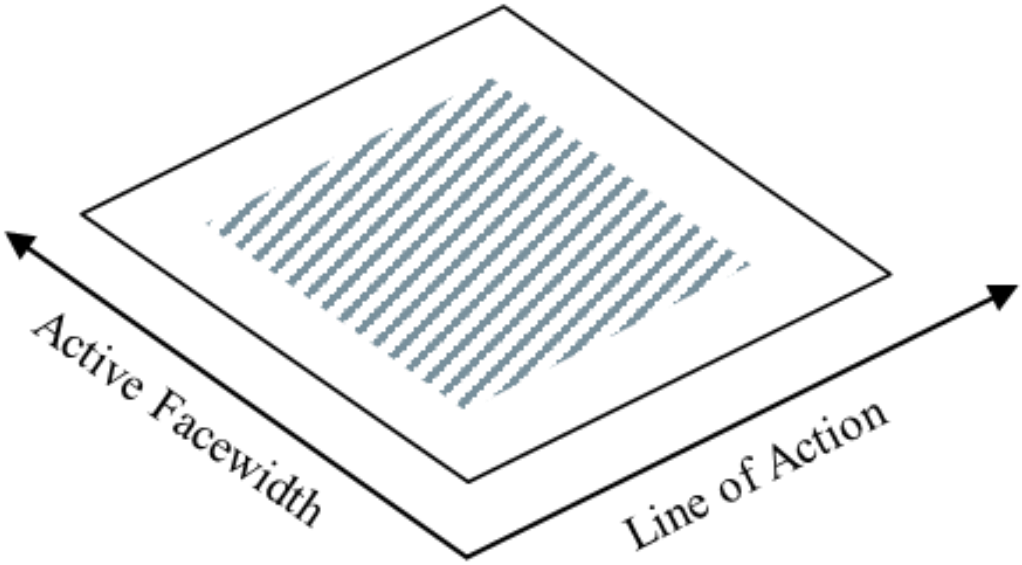

Figure 3.2: 3D Stochastic Model

3D Stochastic Model focused on the same parameters at the on all the points on the hatched region as shown in the figure 3.2.

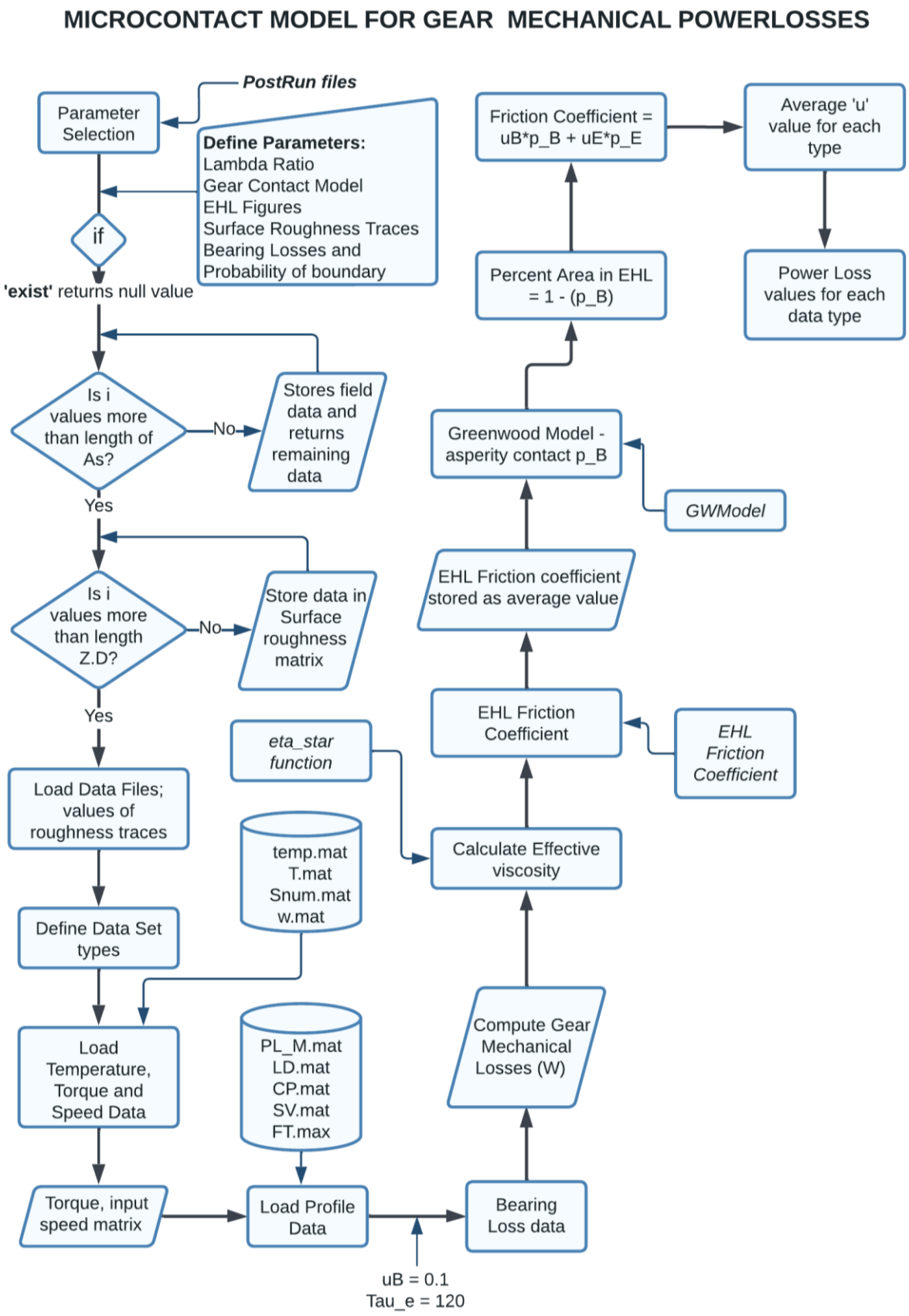

Figure 3.3: Advanced Code Workflow for the Stochastic Model

3.2 INPUTS AND GEAR MODELLING

WindowsLDP (Load Distribution Program) [7] is a quasi-static gear design and analysis tool for external and internal spur and helical gear pairs. This software program has been adapted and used extensively by most of the consortium members as the main gear design and analysis tool. WindowsLDP employs computationally efficient and accurate semi-analytical formulations to compute the load distribution between multiple mating teeth of gears. With the predicted load distribution, it computes the loaded transmission error, root and contact stress distributions, mesh stiffness functions, tooth forces as well as other design evaluation parameters such as lubricant film thickness and surface temperature. WindowsLDP's capabilities also include multi-torque analyses and manufacturing robustness analyses. Tooth modifications of various forms can be entered interactively or can be read from the tooth surface measurements. The results are presented by an interactive graphical user interface that provides the user the flexibility to process and present them in desired formats.

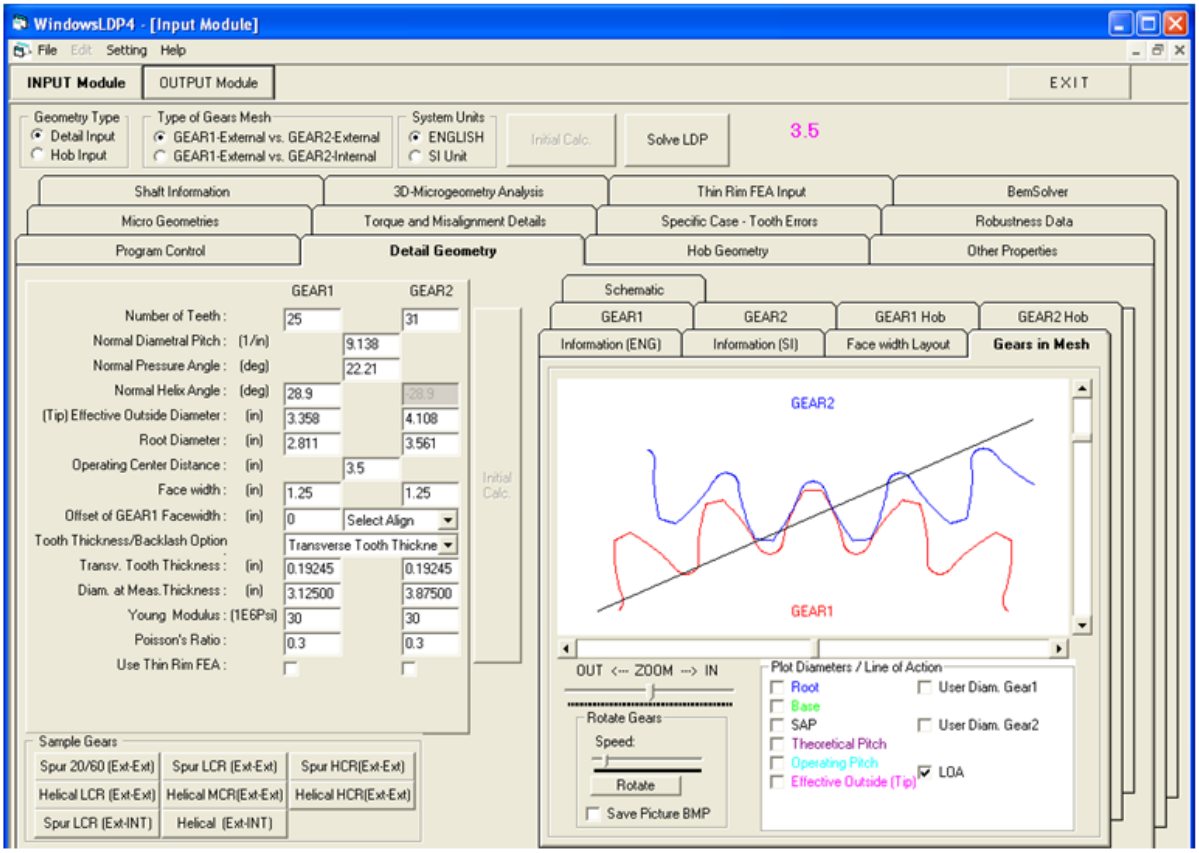

Figure 3.4: Windows LDP Input module interface

WindowsLDP is used to predict the gear loading conditions which are a necessary input in the gear loss model with user input discretization number, which divides the gear tooth contact

surface area into desired number of points and based on that it will output the parameters. WindowsLDP will provide you with a fully loaded matrix for the parameters with number of columns equal to product of discretization number and contact ratio and number of rows equal into length of action across face width (um). As shown in figure 3.7, these are the input we provide to LDP along with the torque, speed, lubricant temperature, and gear roughness values. WindowsLDP program simulates the gear tooth contact outputs .LDO file which is read by the script in the Stochastic Model. This script acquires the necessary input data i.e., load, film thickness, sliding velocity, contact pressure and then generates matrices in an appropriate format that is then used to compute the power loss. Multi-Torque analysis provides use with the mesh power losses that Windows LDP software calculates with the regressed equations derived out of the deterministic model. Thus, along with the measured values, we get Windows LDP power loss values for comparison with our stochastic model. There was a need for a model that processes data directly as compared to the indirect approach for LDP and is fast and gives accurate results.

WindowsLDP is a proprietary software of GearLab, The Ohio State University and without the use of WindowsLDP, we can calculate power loss for singular point that can be represented as average power loss. Without the use of WindowsLDP, it is not possible to acquire the load, film thickness, sliding velocity, contact pressure parameters for every contact point on the gear tooth contact region.

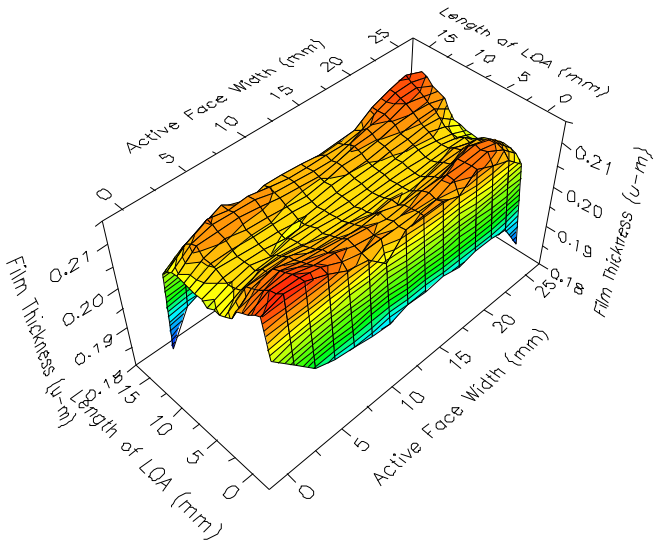

Figure 3.5: Example of data generated in 3D graph format for all contact points in Windows LDP

3.3 ELLIPTICAL CONTACT MODEL METHODOLOGY

The methodology involves modeling a generalized code to compute power loss, film thickness, and friction coefficient between any two contacting surfaces. Initially, the relevant input parameters specific to the experimental conditions are acquired. These parameters cover a wide range of variables, including fluid properties, geometric arrangements, loading scenarios, and material attributes. The input parameters are entered into the universal code when they have been gathered. This code is quite flexible and can be used to examine contact interactions between any two surfaces or gears. Experiment data-validated formulations are incorporated into the code. The formulas used are specifically based on the formulas developed by JB Hamrock and D Dowson for calculating film thickness in elliptical contact situations involving rolling discs or spheres with crowning in elastohydrodynamic lubrication (EHL). Furthermore, suitable formulae for the calculation of Hertzian contact pressure in elliptical contact scenarios are applied. To guarantee these formulas' precision and dependability in forecasting tribological occurrences, validation procedures have been carried out.

By integrating these validated formulations into the code, it becomes a powerful tool for analyzing tribological behavior in diverse scenarios. The code can produce the intended outcomes for the given conditions after the gathered parameters are entered. Key tribological metrics, including power loss, film thickness, and friction coefficient, are included in these outputs. These factors are essential for comprehending and enhancing frictional interactions between contacting surfaces. The code contributes significantly to the advancement of tribology research and useful applications through this methodology.

3.4 ELLIPTICAL CONTACT MODEL INPUTS

The MATLAB function `TribLDM` is a practical tool designed to analyze tribometer experiments, providing valuable insights into the parameters governing friction, wear, and lubrication at material interfaces.

In `TribLDM`, a specific set of input parameters is required to execute the analysis effectively. These parameters are meticulously chosen to capture the essential characteristics of the tribometer setup, and the materials involved. Let us delve into the nature of these input parameters and their role in facilitating meaningful tribological analysis.

Elastic Moduli (E_r, E_d):

The tribometer setup's elastic moduli, E_r and E_d, measure a material's resistance to deformation when stress is applied. E_r is the modulus of elasticity of the roller material, while E_d is the modulus of elasticity of the disc material. These characteristics shed light on how stiff the materials are and how they react to tensile or compressive stresses. E_r and E_d affect the distribution of stress and strain in the materials upon contact, in addition to their function in deformation resistance. Predicting processes like stress transmission, elastic deformation, and possible plastic deformation or material failure requires an understanding of these distribution patterns. As a result, these moduli are essential for evaluating the contacting surfaces' endurance and mechanical performance under various loading scenarios. E_r and E_d also affect interfacial processes including adhesion and abrasion, as well as the development and spread of surface characteristics like scratches and wear marks. Their principles direct the choice of materials for tribometer testing, guaranteeing their compatibility, durability, and anticipated performance under various operating conditions. Therefore, a thorough grasp of Er and Ed makes it easier to make wise judgments when designing tribological systems and makes it possible to forecast how well they would function in certain scenarios.

Poisson's Ratios (v_r, v_d):

The two Poisson's ratios, v_r and v_d, show how different materials react when stretched or compressed in a tribometer configuration. v_d stands for the disc material, which is frequently softer, and v_r for the roller material, which is usually tougher. The amount that materials change shape sideways when pushed or dragged lengthwise is shown by these ratios.

Predicting phenomena such as material elongation, compression, and stress distribution within the contacting surfaces requires an understanding of the lateral strain response. Poisson's ratios also affect material deformation and contact mechanics in tribological interactions, which affects the overall behavior of the machine and its reaction to pressures and forces from the outside world. Furthermore, they influence surface characteristics like wear patterns and the emergence of tribological phenomena like adhesion and abrasion, directing the choice of materials for tribometer testing and guaranteeing suitability, effectiveness, and longevity in practical applications.

Radii of Curvature (R_{rx}, R_{ry}, R_{dx}, R_{dy}):

The surface curvature of the roller material is represented by the radii of curvature, R_{rx} and R_{ry}, in the x and y directions, respectively. R_{dy} indicates the convex or crowning curvature of the disc's surface, whereas R_{dx} and R_{dy} indicate the curvature in the x and y directions, respectively, for the disc material.

These radii give information about the surface geometry and contact mechanics during tribological interactions by characterizing the shape of the contacting surfaces in the tribometer system. R_{dx} and R_{dy} characterize the surface curvature of the disc material, with R_{dy} indicating the presence of any convexity or crown, and R_{rx} and R_{ry} define the surface curvature of the roller material in various directions.

Normal Load (F_n):

The force applied perpendicular to the contacting surfaces is represented by the normal load, F_n. It controls wear processes, true contact area, and contact pressure, which has a significant effect on material wear rates and frictional behavior. It is essential to precisely measure and control the normal load to investigate load-dependent phenomena including adhesion, wear, and frictional reaction.

Angular Velocities (w_r, w_d):

The speeds at which the contacting surfaces in the tribometer arrangement spin are represented by the angular velocities, w_r and w_d. In particular, w_r stands for the roller material's angular velocity and w_d for the disc materials.

These angular velocities have a significant impact on wear rates, frictional behavior, and the efficiency of lubrication by dictating the sliding or rolling speed of the contacting surfaces. The distribution of contact forces and the production and dissipation of heat are influenced by the rotating motion, which controls the relative movement between the surfaces.

The sliding ratio, which ranges from negative to positive values, reflects the ratio of sliding velocity to rolling velocity. In tribometer studies, the rotational speeds of the disc and roller vary linearly while maintaining a constant rolling velocity and varying sliding velocity. With negative ratios showing the opposite direction of sliding and rolling velocities and positive ratios indicating the same direction, this statistic is crucial for characterizing the relative motion of contacting surfaces. We may investigate a variety of frictional regimes and wear

mechanisms, including transitional behaviors like the change from pure rolling to mixed sliding and rolling contact, by adjusting the sliding ratio.

Effective Dynamic Viscosity (n):

The effective dynamic viscosity, denoted as n, represents the fluid's resistance to flow within the tribometer system. The fluid's ease of deformation and movement in response to applied shear stress is measured by this parameter. When it comes to tribological study, the production and stability of lubricating films between the contacting surfaces are largely dependent on the effective dynamic viscosity. Researchers can maximize wear and friction performance and customize the lubrication regime by adjusting the effective dynamic viscosity.

Pressure Viscosity Coefficient (alpha):

The relationship between dynamic viscosity and pressure in the lubricating film between contacting surfaces is described by the pressure viscosity coefficient, alpha. This coefficient measures how viscosity varies under pressure and how that affects the lubricant film's thickness and ability to support loads. While a lower alpha denotes a less noticeable effect, a larger alpha implies a more notable rise in viscosity with pressure, resulting in thicker and more resilient films. The accurate modeling of lubrication regimes made possible by alpha calibration makes it easier to predict frictional behavior under different circumstances.

A range of significant input parameters required for carrying out tribometer experiments and examining friction at material interfaces are gathered by the TribLDM function. This function yields useful outputs including minimum film thickness, contact surface, and sliding velocities at that point by considering material properties, geometric setups, loading conditions, and fluid characteristics.

CHAPTER FOUR: RESULTS AND DISCUSSIONS

4.1 RESULTS - GEAR POWER LOSS MODEL

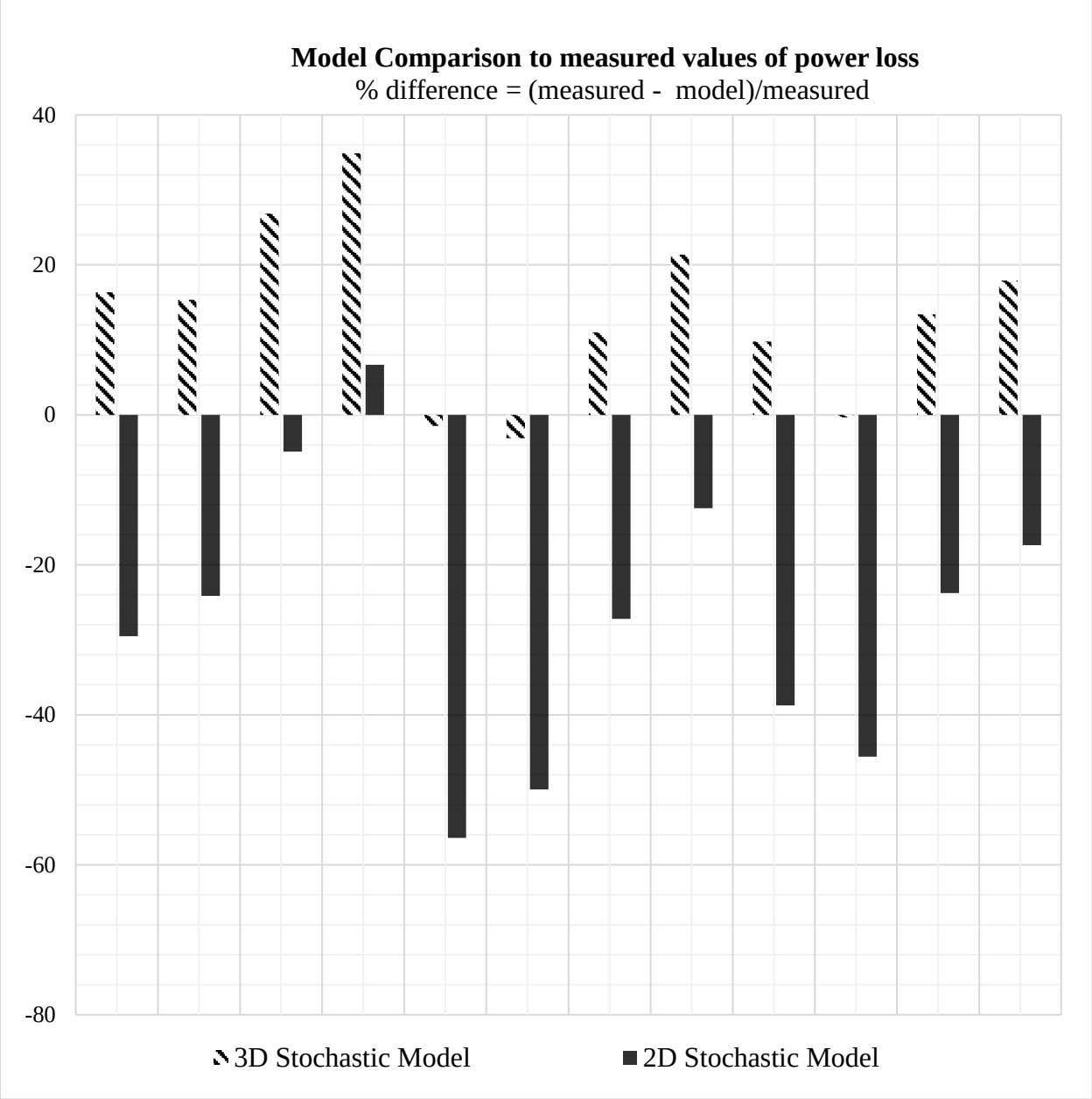

Figure 4.1: Comparison to stochastic models with measured data for power loss

Figure 4.1 shows percent difference between the measured power losses from the test setup in [5] and the power loss data obtained from 3D stochastic model and the 2D Stochastic model as referred in the chapter 3. From results, we can see that the 3D Stochastic model is more accurate for a large range of data.

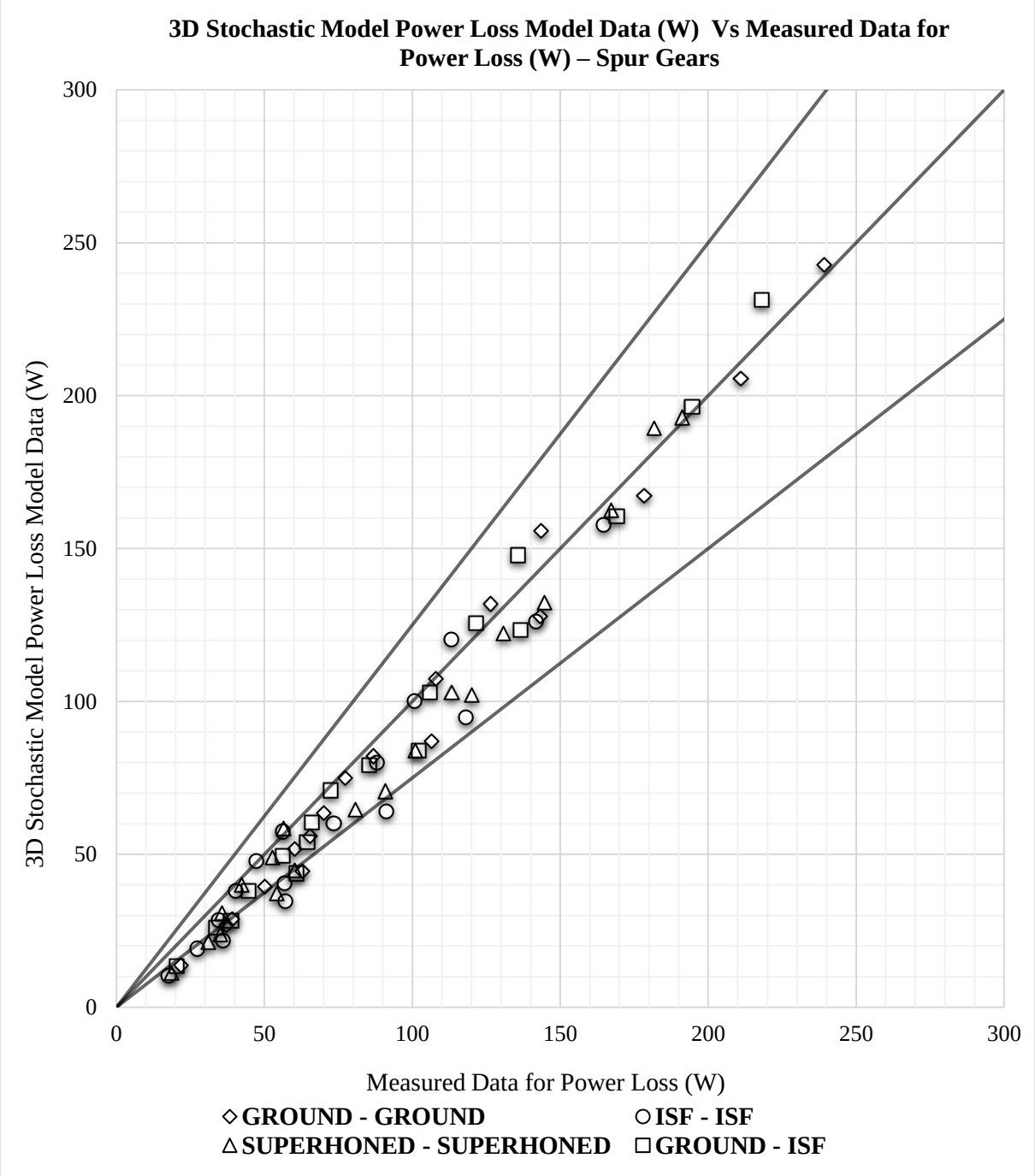

Figure 4.2: 3D Stochastic Model Power Loss Model Data (W) Vs Measured Data for Power Loss (W) – Spur Gears

From the figure, it is evident that the measured and the model power losses are similar and the power losses computed with the Stochastic model for spur gears are in the desired error range for all the given cases of torque, speed and surface roughness. We can observe that at lower values, few points may be outside the -25% error range, however the difference between the power losses is not significant (i.e., difference of 5-7 watts).

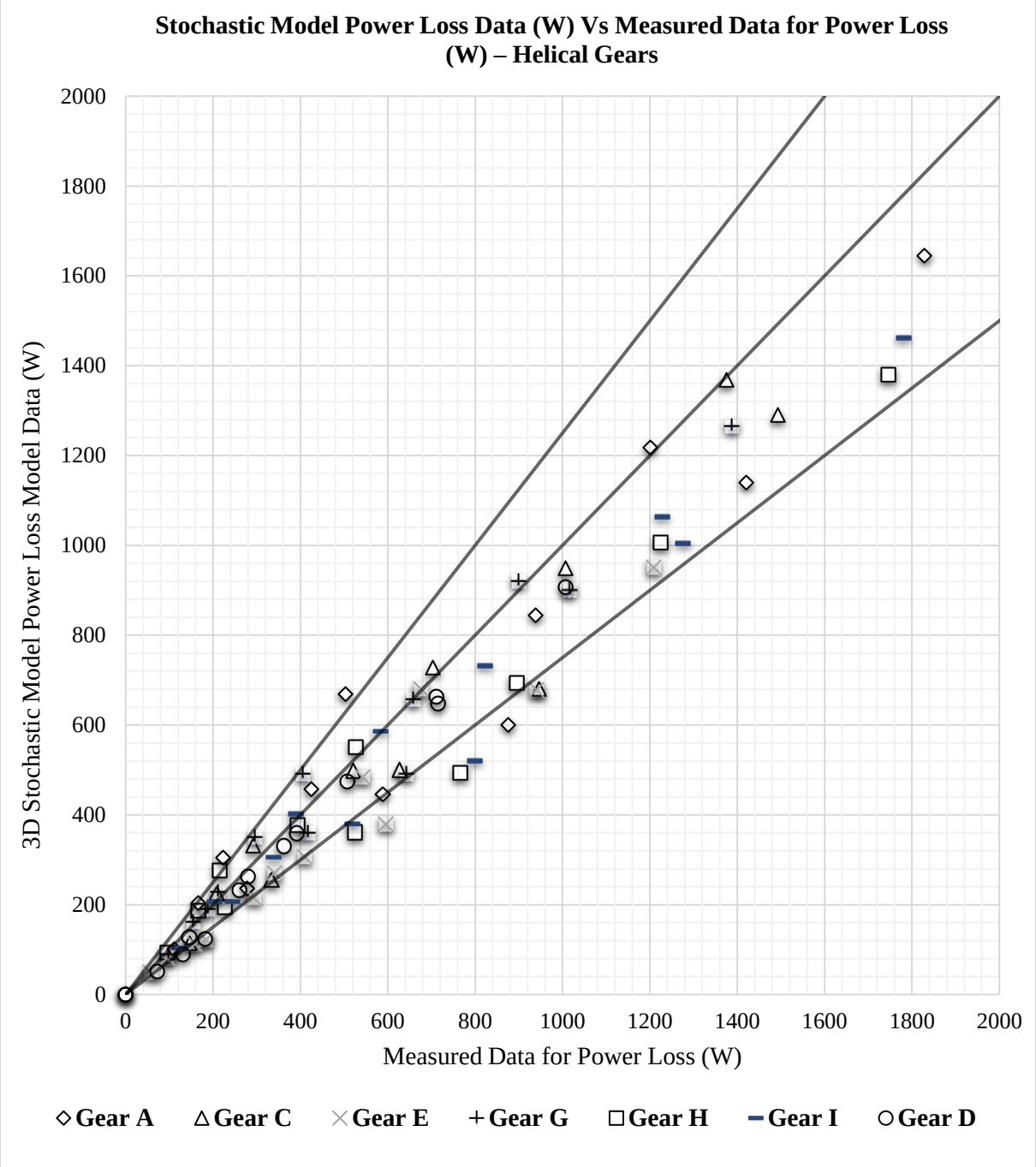

Figure 4.3: Stochastic Model Power Loss Data (W) Vs Measured Data for Power Loss (W) – Helical Gears

The power losses calculated using the stochastic model for Helical gears from [4] are within the intended error range for all of the given scenarios of torque, speed, and surface roughness, as can be seen from the figure, which also shows similarities between the observed and model power losses. Although a small number of points may fall beyond the -25% error range at lower values, the difference in power losses is not statistically significant.

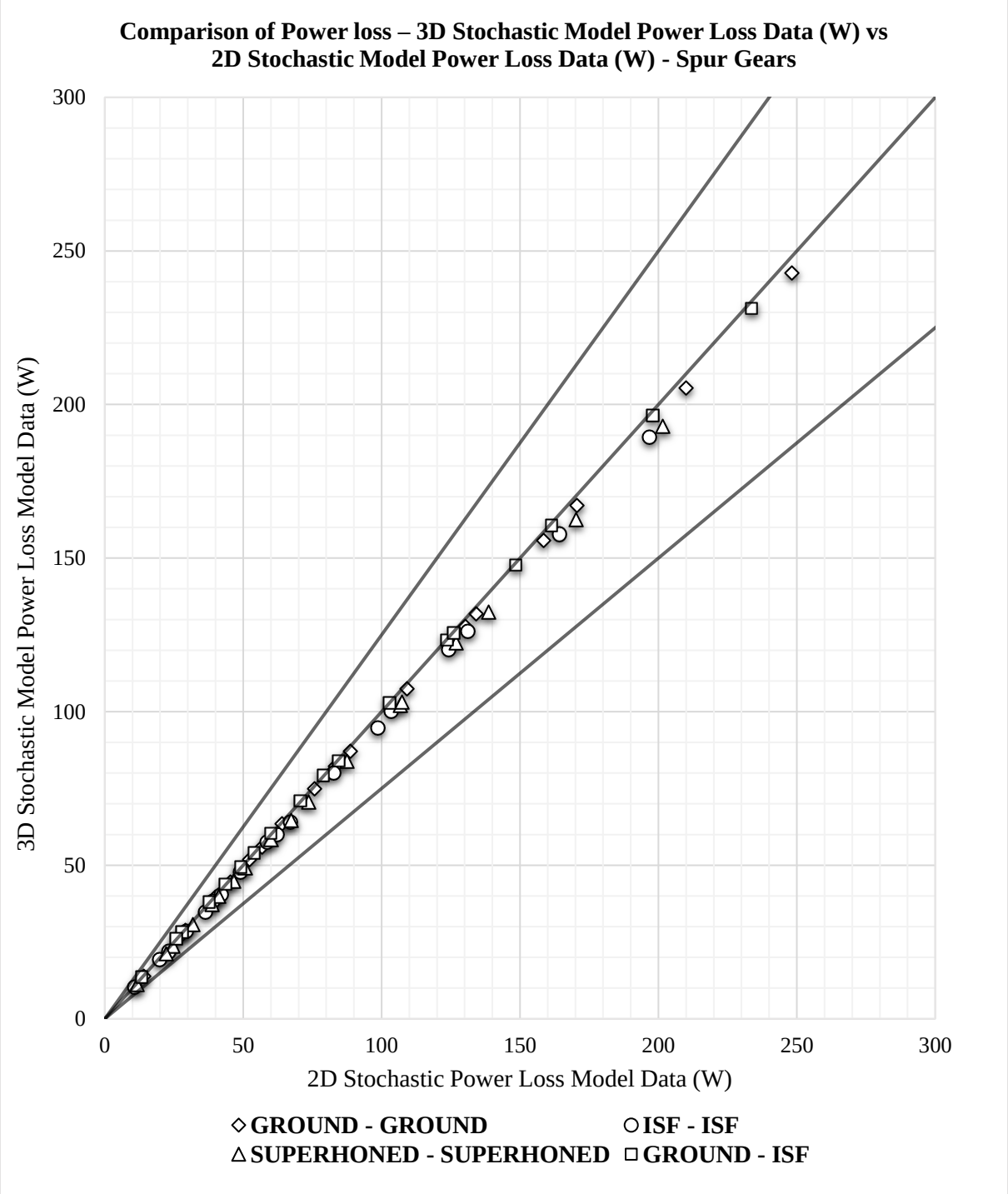

Figure 4.4: Comparison of Power loss – 3D Stochastic Model Power Loss Data (W) vs 2D Stochastic Model Power Loss Data (W) - Spur Gears

Figure 4.4 shows comparison between the 2D and the 3D Stochastic model for spur gears and both the models show mostly identical results for all the cases and hence majority of points lie on the ideal line with a slight deviation with 2D Stochastic model predicting power loss values on the higher side.

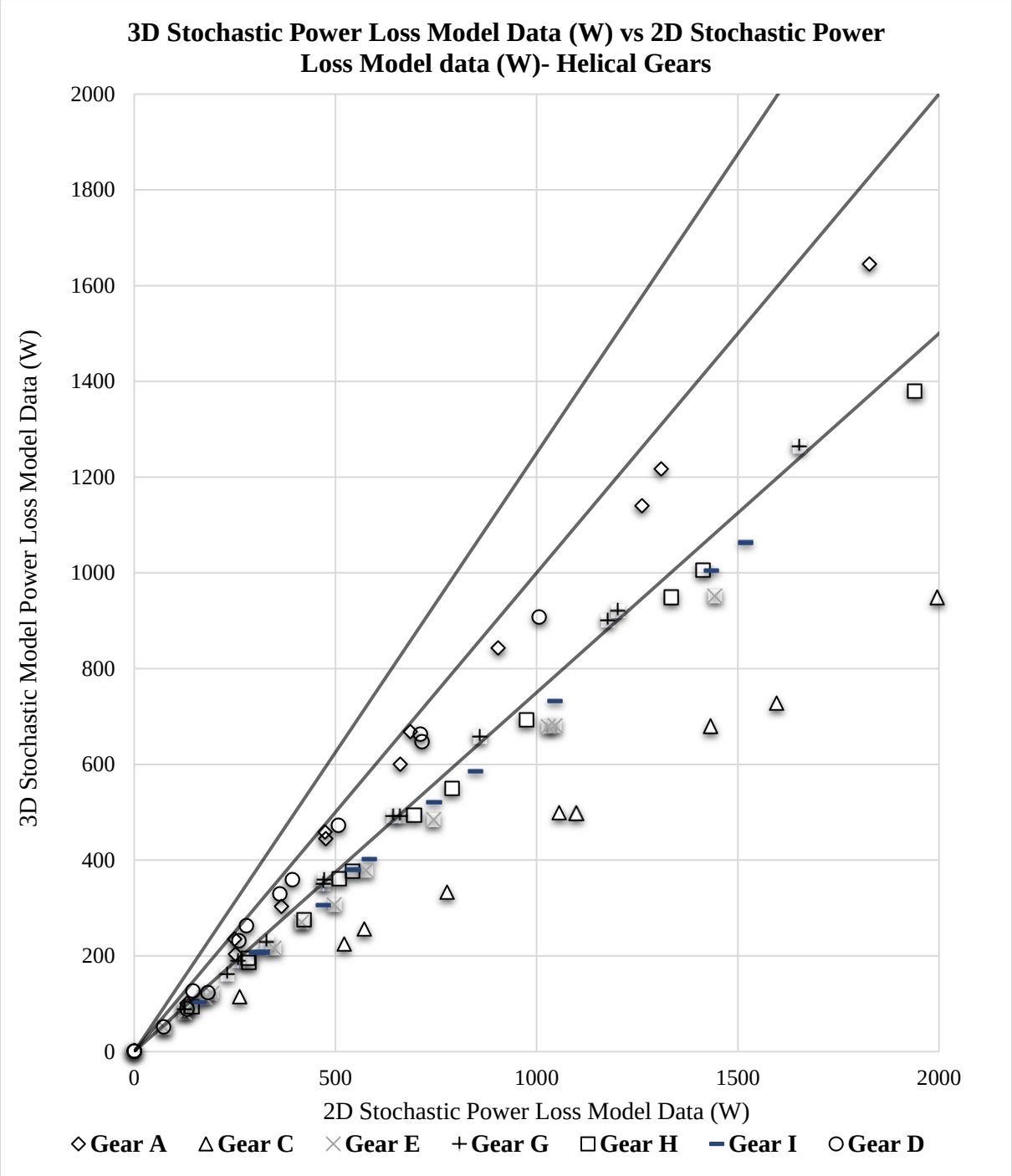

Figure 4.5: 3D Stochastic Power Loss Model Data (W) vs 2D Stochastic Power Loss Model data (W)- Helical Gears

The plot in figure 4.5 shows comparison of power loss values from 2D and the 3D Stochastic model and we can see that the difference is too large with 3D stochastic model being more accurate as seen in the figure 4.1. The inaccuracy of 2D Stochastic model prompted the need for development of 3D Stochastic model in first place, addressing the issue of covering points on the entire contact region.

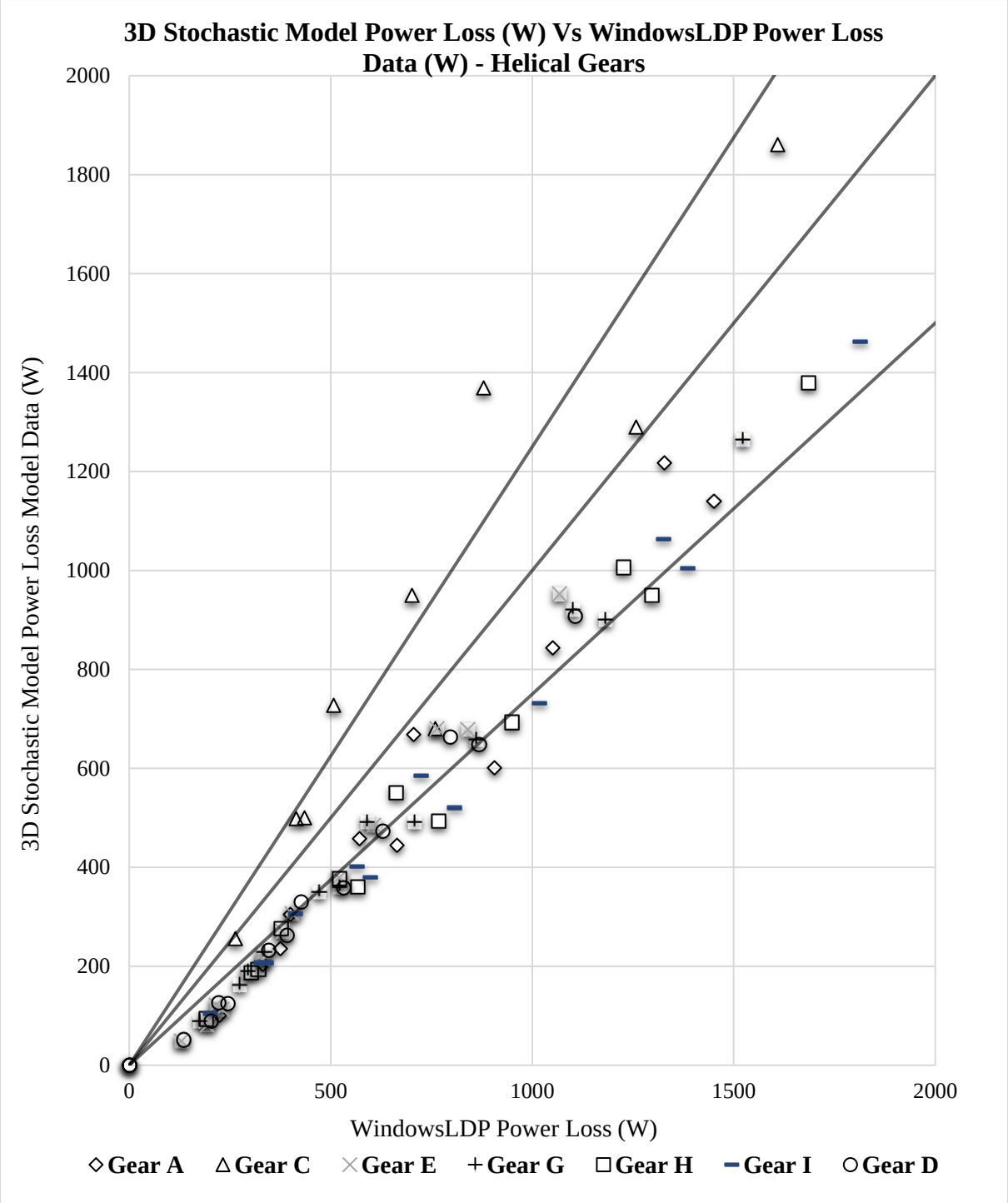

Figure 4.6: 3D Stochastic Model Power Loss (W) Vs WindowsLDP Power Loss Data (W) - Helical Gears

Figure 4.6 shows comparison between the 3D Stochastic power loss model and power loss data obtained from the regressed model of WindowsLDP for same values of torque and speed. WindowsLDP has a general trend of producing power loss values on a higher side.

4.2 RESULTS - ELLIPTICAL CONTACT POWER LOSS MODEL

a. MILPRF Oil

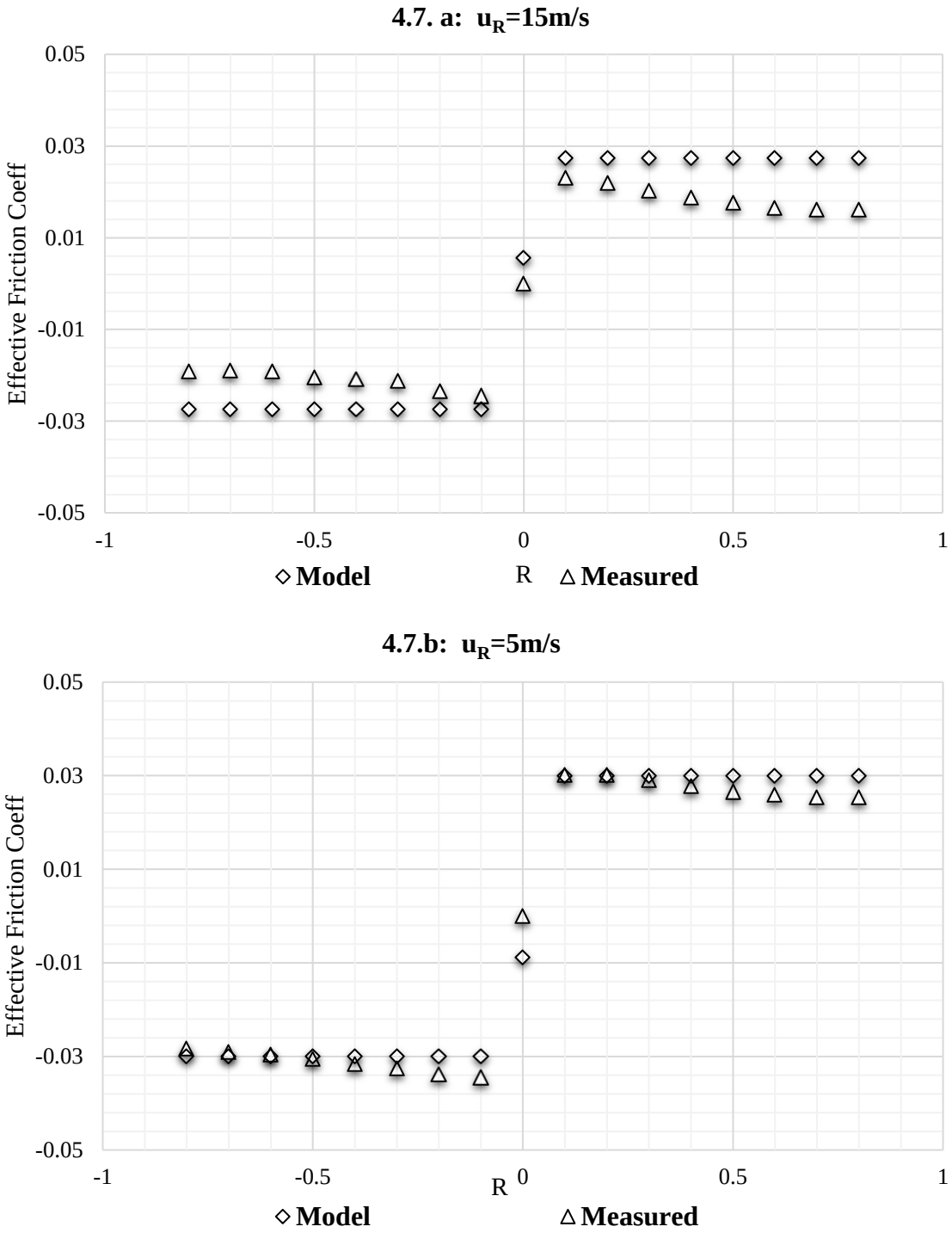

Figure 4.7: Comparison to stochastic models with measured data for Effective friction Coefficient of MILPRF, (a) = 15 m/s (b) = 5 m/s

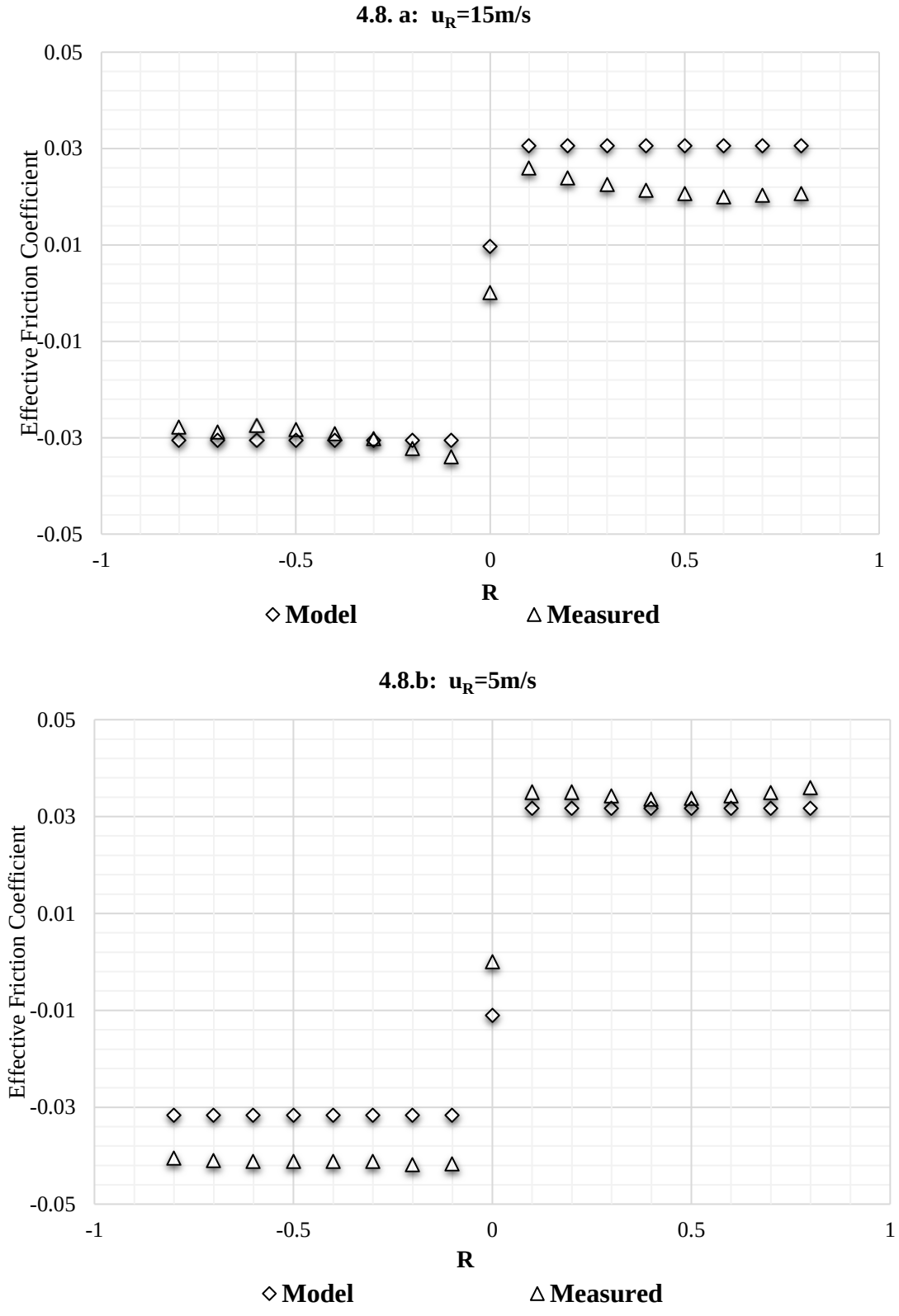

Figure 4.8: Comparison to stochastic models with measured data for Effective friction Coefficient of 80W90, (a) = 15 m/s (b) = 5 m/s

The figure 4.7 compares the MILPRF lubricant's effective friction coefficient at a rolling speed of 5 m/s and 15 m/s under a normal load of 1900N with the measured values obtained from the test specimen and Fig 4.8 compares the 80W90 lubricant's effective friction coefficient at a rolling speed of 5 m/s and 15 m/s under a normal load of 1900N with the measured values obtained from the test specimen. The model's predictions for the friction coefficient turned out to be higher than what we observed in our tests. This discrepancy likely stems from two main factors:

Firstly, the threshold value used to calculate the effective viscosity of the lubricant is set too low for the specific lubricants employed in our twin-disk tribometer setup. Essentially, the model underestimates how thick the lubricant layer needs to be to reduce friction effectively. Secondly, as the slide to roll ratio increases it causes rise in temperature as thus the viscosity properties of the oil changes as per temperature which is not taken into account for the model which causes deviation from the experimental values at higher value of slide to roll ratio.

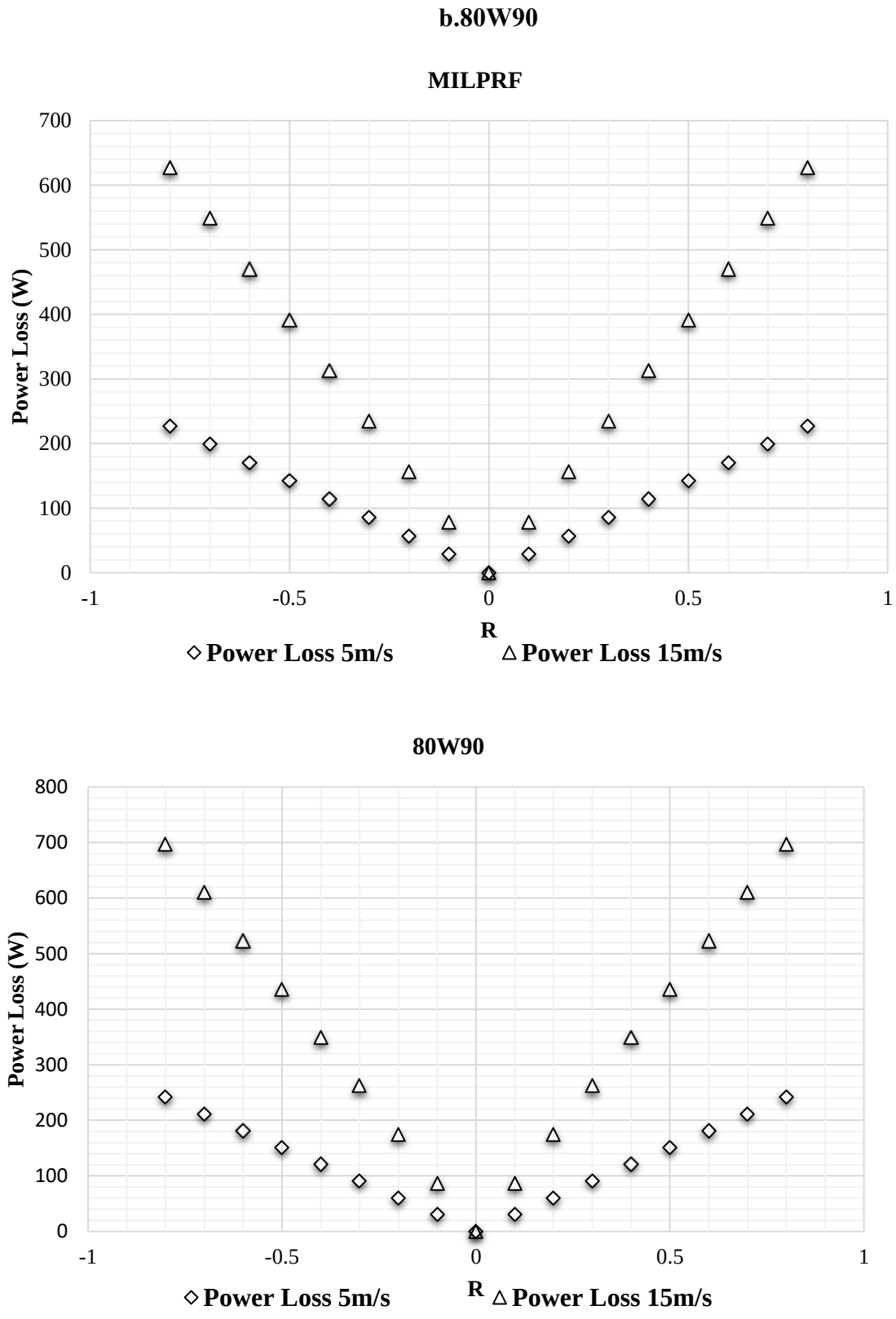

Figure 4.9: Comparison to Power Loss with Rolling Ratio for Rolling Speed 5 m/s and 15 m/s, (a) MILPRF (b) 80W90

The figure 4.9 gives values of Power loss for the lubricants MILPRF and 80W90 respectively corresponding to their respective Rolling Ratios. Following are some of the outcomes: Rolling contact represents ideal movement where surfaces roll over each other without relative sliding. This minimizes friction and energy dissipation. Sliding contact occurs when there's a difference in the rolling velocities of the contacting surfaces. This creates friction and results in power loss. In our case, the slide-to-roll ratio (part R) is defined as the ratio of sliding velocity to constant rolling velocity. Since the rolling velocity is constant, variations in sliding velocity will directly cause the roll ratio to change. As the slide to roll ratio increases, the relative sliding velocity between the surface's increases. This increases the frictional forces and consequently, the power loss due to friction. It was found that the curve is symmetric to that of X axis and linear in nature. However, it is essential to note that the relationship between power loss and rolling ratio may not always follow a linear pattern. Comprehending how power loss changes with the rolling ratio is vital for improving the performance of systems that use elliptical contacts, like gears and bearings. By pinpointing the best rolling ratio and its associated power loss, engineers can boost efficiency, decrease damage, and extend the lifespan of these components.

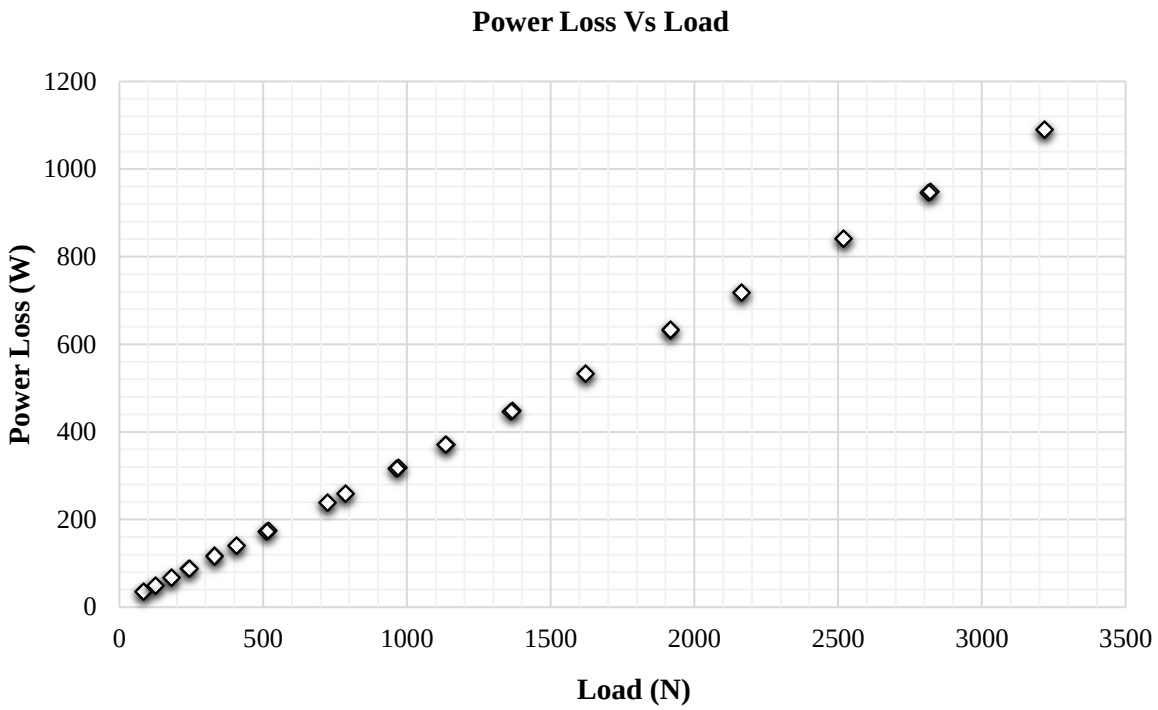

Figure 4.10: Elliptical Contact Power Loss vs Load

when we apply more weight or pressure on the surfaces in contact, the lubricant film between them gets squeezed thinner. Consequently, the reduced film thickness shifts the lubrication regime towards boundary lubrication, where friction increases due to decreased lubrication effectiveness which causes increase in the power loss. A similar trend can be seen from figure 4.10.

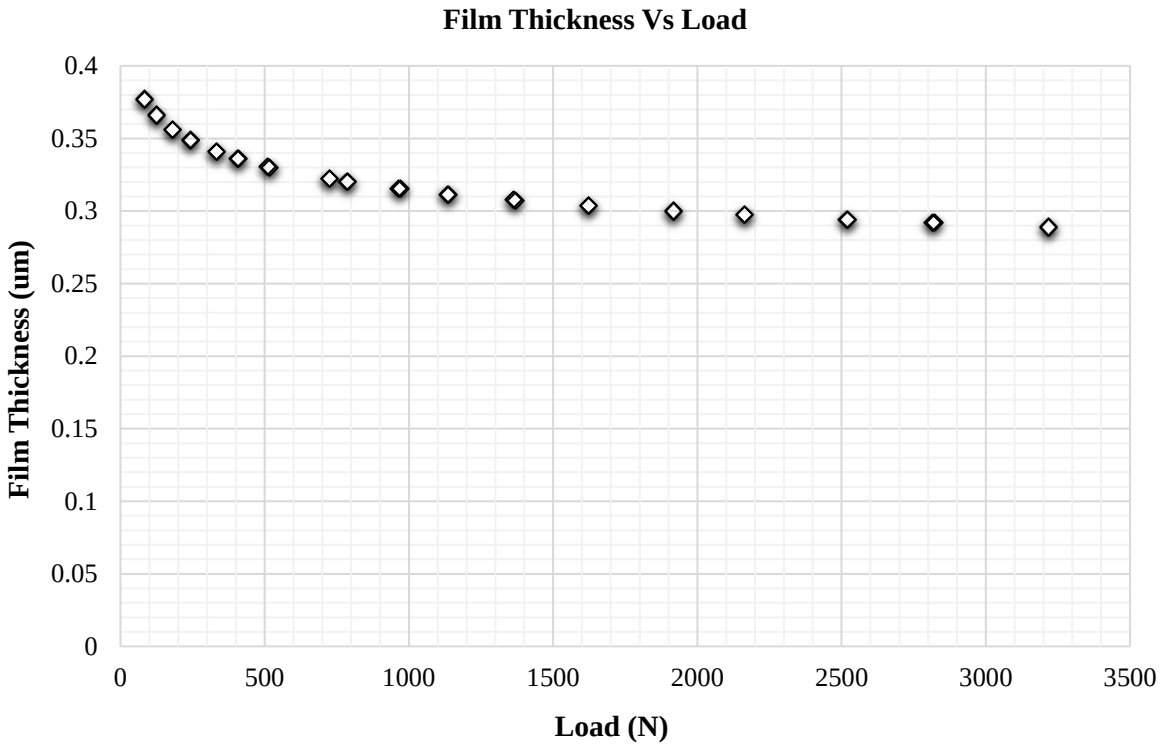

Figure 4.11: Minimum Film Thickness vs Load

The observed trend in the graph, where film thickness decreases with increasing load but stabilizes beyond a certain point, can be attributed to several factors. At lower loads, the film and substrate may undergo significant elastic deformation, leading to a rapid decrease in film thickness. As the load increases, the material might reach a state where further deformation is limited by its elastic properties. Additionally, in lubricated systems, hydrodynamic effects play a crucial role. At higher loads, the film may reach an equilibrium thickness where the pressure build-up from the fluid's viscosity counterbalances the applied load, resulting in a stable film thickness. The material's intrinsic properties, such as hardness and compressibility, also contribute to this phenomenon. Once the material is compressed to a certain extent, its resistance to further compression increases, making the reduction in thickness less pronounced. Furthermore, surface interactions at higher loads could lead to the formation of a more robust, stable film layer, preventing significant thinning despite the increasing load. These factors together explain the initial rapid decrease in film thickness followed by stabilization, as depicted in the figure 4.11

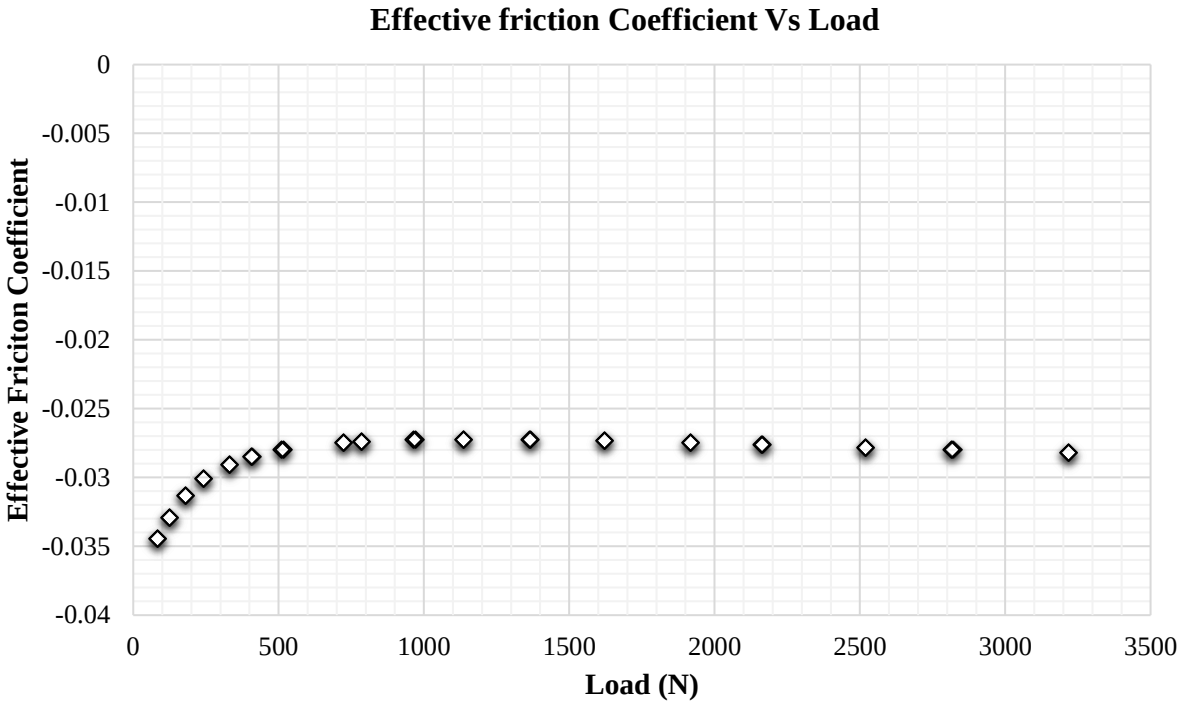

Figure 4.12: Effective Friction Coefficient vs Load

The effective friction coefficient starts at a more negative value and increases (becomes less negative) as the load increases up to around 500 N. After approximately 500 N, the effective friction coefficient stabilizes around a value slightly below -0.03. This suggests that beyond a certain load, the effective friction coefficient remains relatively constant despite increasing load. The stabilization of the coefficient at higher loads might indicate a threshold beyond which the lubricant's frictional properties do not change significantly with increasing load. It must be noted that the negative value of coefficient of friction simply denotes the velocity direction.

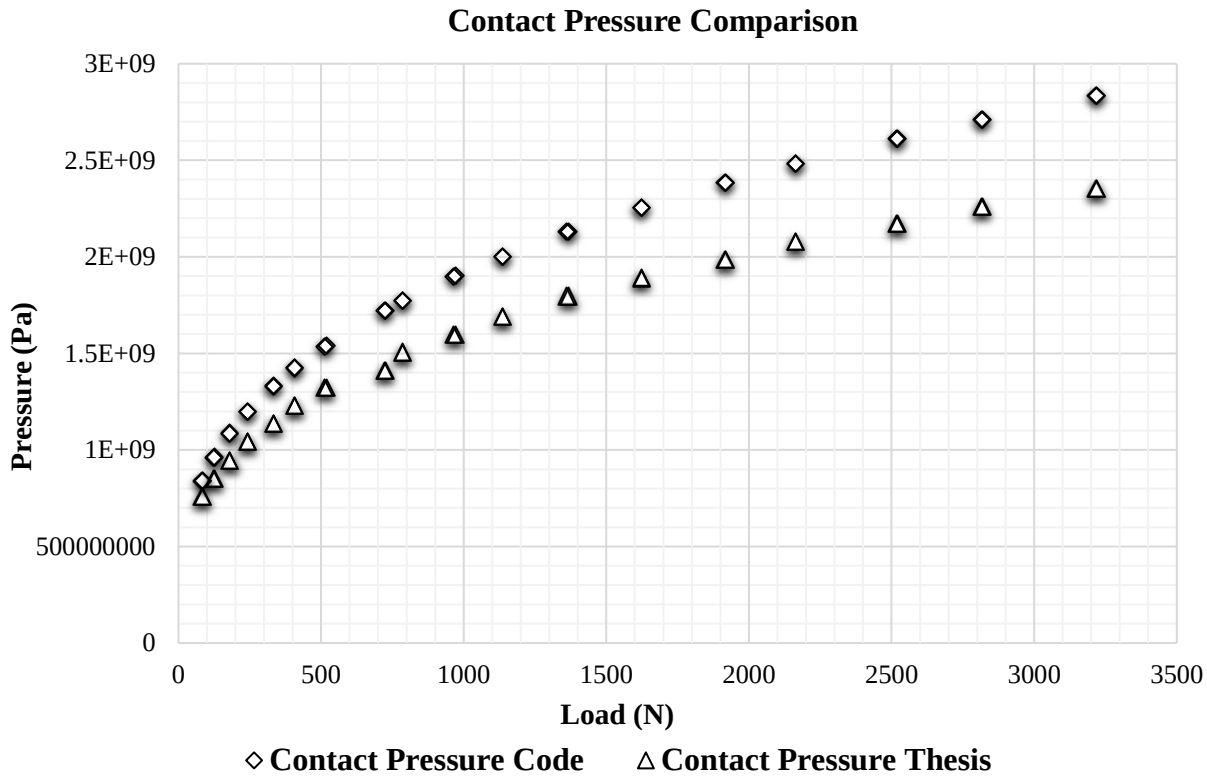

Figure 4.13: Contact Pressure Comparison between the Stochastic model and the formulation used in thesis

The above graph illustrates the relationship between contact pressure and load from the results obtained via both, the model developed and the referred thesis. It can be observed that both show similar a similar trend. The difference in values can be attributed to the variation in behaviour of the lubricant as its temperature increases with increasing load, as this behaviour is not simulated by the model.

CHAPTER FIVE: CONCLUSIONS AND FUTURE SCOPE

5.1 CONCLUSIONS – GEAR POWER LOSS MODEL

The investigation into the performance of helical and spur gears has provided valuable insights into their behaviour and power loss calculations. The experimental results shed light on various aspects, such as error ranges, roughness influence, and the efficacy of stochastic model. This comprehensive conclusion summarizes the key findings and their implications, while also highlighting potential areas for future research and development.

1. Helical Gears

The analysis of helical gears demonstrated a favourable trend, with most data points falling within the acceptable error range of +- 25% as seen in the figure 4.3. This finding validates the effectiveness of the 3D Stochastic model used for power loss calculations. Figure 4.1 shows the percentage difference between the power loss values predicted by 3D and 2D Stochastic model and from that, we can conclude that 3D Stochastic model is more accurate than the 2D Stochastic model.

From figure 4.5, we can see that the 2D Stochastic model had a trend of predicting power loss values more than or equal to 3D Stochastic model. This inaccuracy in 2D Stochastic model is due to the simplified approach which may not work for helical gears due to non-symmetric nature along Line of Action. 3D Stochastic model includes all the contact points for calculation of power loss and hence, it is more accurate. In figure 4.6, we can see that the 3D Stochastic model predicts value like power loss values predicted by WindowsLDP regressed deterministic model.

2. Spur Gears

The analysis of spur gears revealed results in line, as most data points fell within the acceptable error range as seen in figure 4.2. This consistent behaviour between the two gear sets provides valuable insights into their comparative performance. Like helical gears, the power loss calculations for spur gears aligned well with measured power loss values. From figure 4.4, we can see that 3D Stochastic model and 2D Stochastic model predicted same value as the contact geometry for spur gears is symmetric and easy to compute.

The findings from this study carry significant implications for the design and optimization of helical and spur gears. The results demonstrate the importance of incorporating accurate roughness data in power loss calculations to reduce uncertainty and enhance precision. Furthermore, the results from Windows LDP indicate that the software could be a valuable tool for initial design considerations and quick assessments, especially for spur gears. Indeed, the stochastic model has demonstrated its viability by providing results that fall within the accepted error range. This suggests that the model can predict gear performance with a reasonable level of accuracy. Given its favourable performance, it can serve as a valuable tool in conjunction with the WindowsLDP for verification and validation purposes.

5.2 CONCLUSIONS – ELLIPTICAL CONTACT POWER LOSS MODEL

The examination of elliptical contacts' performance has yielded significant insights into their behaviour and power dissipation computations. The empirical findings illuminate several facets, including minimum film thickness, power dissipation, contact pressure, and normal load. This thorough synopsis encapsulates the primary discoveries and their ramifications, while also underscoring potential avenues for further research and advancement. Following are some of the findings:

Comparison of the Measured and the Model Values of Effective friction Coefficient:

The Plot no. compares the MILPRF lubricant's effective friction coefficient at a rolling speed of 5 m/s and 15 m/s under a normal load of 1900N with the measured values obtained from the test specimen. The model's predictions for the friction coefficient turned out to be higher than what we observed in our tests. This discrepancy likely stems from two main factors:

- Firstly, the threshold value used to calculate the effective viscosity of the lubricant is set too low for the specific lubricants employed in our twin-disk tribometer setup. Essentially, the model underestimates how thick the lubricant layer needs to be to reduce friction effectively.
- Secondly, when we apply more weight or pressure on the surfaces in contact, the lubricant film between them gets squeezed thinner. Consequently, the reduced film thickness shifts the lubrication regime towards boundary lubrication, where friction increases due to decreased lubrication effectiveness.

Comparison of Power Loss and the Rolling Ratio:

The plot number gives values of Power loss for the lubricants MILPRF and 80W90 respectively corresponding to their respective Rolling Ratios. Following are some of the outcomes: Rolling contact represents ideal movement where surfaces roll over each other without relative sliding. This minimizes friction and energy dissipation. Sliding contact occurs when there's a difference in the rolling velocities of the contacting surfaces. This creates friction and results in power loss. In our case, the slide-to-roll ratio (part R) is defined as the ratio of sliding velocity to constant rolling velocity. Since the rolling velocity is constant, variations in sliding velocity will directly cause the roll ratio to change. As the slide to roll ratio increases, the relative sliding velocity between the surface's increases. This increases the frictional forces and consequently, the power loss due to friction. It was found that the curve is symmetric to that of X axis and linear in nature. However, it is essential to note that the relationship between power loss and rolling ratio may not always follow a linear pattern. Comprehending how power loss changes with the rolling ratio is vital for improving the performance of systems that use elliptical contacts, like gears and bearings. By pinpointing the best rolling ratio and its associated power loss, engineers can boost efficiency, decrease damage, and extend the lifespan of these components.

5.3 FUTURE SCOPE

To build on the insights gained from this study, future research should focus on several key areas:

1. **Advanced Analysis Methods**: Develop and implement more sophisticated analysis techniques that can handle numerical limitations and cater to the unique characteristics of various gear types.
2. **Enhanced Roughness Measurement:** Improve roughness measurement techniques to provide accurate and comprehensive data for power loss calculations.
3. **Robust Software Solutions:** Continuously improve gear analysis software, such as Windows LDP, to handle diverse gear configurations and offer more detailed outputs for enhanced reliability.
4. **Comparative Studies:** Conduct more in-depth comparative studies between different gear types and analysis methods to identify their strengths and limitations in various scenarios.

References

1. Li S, Kahraman A. “A method to derive friction and rolling power loss formulae for mixed elastohydrodynamic lubrication.” J Adv Mech des Syst Manuf 2011;5(4): 252–63.
2. Greenwood JA, Williamson JBP. “Contact of nominally flat surfaces”. Proc R Soc Lond Ser A Math Phys Sci 1966;295(1442):300–19.
3. Tallian T. “The theory of partial elastohydrodynamic contacts”. Wear 1972;21: 49–101.
4. I. Hong, E. Aneshansley, K. Chaudhury, D. Talbot, “Stochastic microcontact model for the prediction of gear mechanical power loss”, Tribology International 183 (2023) 108413.
5. Aarthy Vaidyanathan, “An Experimental Investigation of Helical Gear Efficiency”, Graduate Thesis, The Ohio State University, 2009.
6. Bartelmus, Walter & Zimroz, Radoslaw. (2008). “Nr 123 BELT CONVEYOR DRIVING SYSTEM VIBRO–ACOUSTIC SEVERITY REDUCTION BY CONDITION BASED MAINTENANCE”. Prace Naukowe Instytutu Górnictwa Politechniki Wrocławskiej, https://www.researchgate.net/publication/269399839_Nr_123_BELT_CONVEYOR_DRIVING_SYSTEM_VIBRO-ACOUSTIC_SEVERITY_REDUCTION_BY_CONDITION_BASED_MAINTENANCE
7. Windows-LDP, Load Distribution Program, The Gear and Power Transmission, Research Laboratory, The Ohio State University, Columbus, Ohio, v4.14.0
8. Dowson, D., and Toyoda, S. (1978), “A Central Film Thickness Formula for Elastohydrodynamic Line Contacts”, Proceedings of the 5th Leeds-Lyon Symposium, London, pp. 60–65.
9. Contact Mechanics, K. L. Johnson, Cambridge University Press, 1987
10. H.K. Yoon, A.J. Ghajar, “A note on the Powell-Eyring fluid model” International Communications in Heat and Mass Transfer, Volume 14, Issue 4, July–August 1987, pp. 381-390
11. J.I. McCool , “Relating Profile Instrument Measurements to the Functional Performance of Rough Surfaces.” J. Tribol. Apr 1987, 109(2): 264-270 (7 pages), https://doi.org/10.1115/1.3261349

12. I. Hong, E. Aneshansley, D. Talbot, “Mechanical Power Loss of Spur Gears Subject to various Surface Finish Pairings”, AGMA Technical Paper 2022.
13. “Probing the molecular design of hyper-branched aryl polyesters towards lubricant applications” - Scientific Figure on ResearchGate. Available from: https://www.researchgate.net/figure/A-Stribeck-curve-and-illustrations-of-the-3-lubricant-regimes-occurring-simultaneously-in_fig4_289495693
14. Wang, Q.J., Zhu, D. (2013). Hertz Theory: Contact of Cylindrical Surfaces. In: Wang, Q.J., Chung, YW. (eds) Encyclopedia of Tribology. Springer, Boston, MA. https://doi.org/10.1007/978-0-387-92897-5_491
15. https://tribos.wordpress.com/tag/contact-mechanics/
16. R. J. Chittenden, D. Dowson, J.F Dunn, C. M. Taylor, “A theoretical analysis of the isothermal elastohydrodynamic lubrication of the concentrated contacts. (I. & II.)” Proc. R. Soc. Land. A 397, 245-269 (1985)
17. “Samuel Shon, “An experimental study on the impact of various surface treatments on friction, scuffing and wear characteristics of lubricated rolling-sliding contacts.” Graduate Thesis, The Ohio State University (2012)
18. Greenwood, James. (1985). “Analysis of Elliptical Hertzian Contacts”, Tribology International 30 (1997) pp. 235-237.
19. “Machine Learning for Film Thickness Prediction in Elastohydrodynamic Lubricated Elliptical Contacts” - Scientific Figure on ResearchGate. Available from: https://www.researchgate.net/figure/The-contact-geometry-of-a-an-actual-elliptical-contact-and-b-a-reduced-elliptical_fig1_375853773
20. Marian, Max, Marcel Bartz, Sandro Wartzack, and Andreas Rosenkranz. (2020) "Non-Dimensional Groups, Film Thickness Equations and Correction Factors for Elastohydrodynamic Lubrication: A Review" Lubricants 8, no. 10: 95. https://doi.org/10.3390/lubricants8100095
21. “Combined effect of boundary layer formation and surface smoothing on friction and wear rate of lubricated point contacts during normal running-in processes” - Scientific Figure on ResearchGate. Available from: https://www.researchgate.net/figure/Schematic-of-mixed-lubrication_fig1_327471085